Bijan Bayat Mokhtari

Development of an Intelligent Safety Gear System for High-Rise Elevators

Author Bijan Bayat Mokhtari

Title of thesis Development of an Intelligent Safety Gear System for High-Rise Elevators

Degree programme Degree Programme in Mechanical Engineering

Major/minor Mechanical Engineering   **Code** IA3027

Thesis supervisor Kalevi Ekman

Thesis advisor(s) D.Sc. Mikko Puranen

Date 27.11.2017   **Number of pages** 49 + 17   **Language** English

Abstract

Elevators have been a key element of buildings, especially tall buildings, since their widespread use began in the 19th century. As a matter of fact, high-rise buildings would not have existed without elevators. Elevators have a myriad of safety features and devices to ensure a safe journey for the passengers. One of these devices is the safety gear. Safety gears are emergency brakes that stop speeding elevators by gripping the guide rails. They are adjusted for a safe deceleration range by the technician during installation and exert a constant force. Due to their purely mechanical nature, once triggered, the safety gear is currently unable to actively adjust the braking force to counteract vibrations, to decelerate at different rates, or to stop the elevator at the closest landing. Therefore, the emergency braking event can be harsh and noticeable, leaving the passengers stuck in the elevator shaft after the braking event.

This thesis aims to develop an intelligent safety gear system that is able to bring the elevator to a stop with a safe and adjustable deceleration rate. This was achieved by first, modeling a computer simulation of a small-scale elevator to be able to quickly simulate different braking event scenarios. Second, a small-scale elevator test rig was constructed to test the computer simulation with physical components. The test rig was validated by comparing its results with KONE's high-rise safety gear test.

The control system developed was able to safely stop the moving mass with the desired deceleration and a great deal of control over other parameters. Further development of the system could lead to a safer, more comfortable, and energy efficient elevator ride.

Keywords Elevator, safety gear, emergency brake, control system

Acknowledgements

Table of Contents

List of Abbreviations

SG	Safety Gear
PID	Proportional, Integral, and Derivative
CW	Counterweight
OSG	Overspeed Governor
RDF	Recall Drive Feature
G (Gs)	Gravitational acceleration equal to 9.81m/s². Not to be confused with Giga Seconds
N	Newtons
kg	Kilo grams
m	Meters
s	Seconds
CNC	Computer Numerical Control
ul	Unitless
mm	millimeters
Nmm	Newton millimeter
mH	MilliHenry
RIO	Reconfigurable Input/output
FPGA	Field Programable Gate Array
VI	Virtual Instrument
ASIC	Application-Specific Integrated Circuit
SGAT	Safety Gear Activation Test

CHAPTER 1

1   Introduction

1.1 Background

Elevators are a necessity in our modern life, since they enable quick and effortless flow of people and goods. Indeed, without elevators, high-rise buildings would not exist. Similar to other vehicles that transport people, safety is of utmost importance in elevators. An integral part of the elevator is its emergency brake, hereafter referred to as the Safety Gear (SG). The sole purpose of the SG is to quickly and securely bring the elevator car to a halt in case of an emergency. The SG is triggered when overspeed is detected and is not used in normal stopping conditions. Thus, safety gears serve as fail-safe mechanical devices that are not actively controlled. When engaged, the safety gear currently used in most elevators exerts a constant force for almost the whole duration of the braking event in order to stop the moving car (1) . This occurs regardless of the velocity, mass, rate of deceleration, or the location of the car in the elevator shaft. Although adjusted for a safe deceleration, the braking event is still uncomfortable for the passengers and can even lead to injuries if the passengers lose their balance. Moreover, because the stopping location of the car is irrelevant to the function of the safety gear, the car could end up becoming positioned almost anywhere along the shaft, possibly between landings, thereby making rescue more difficult.

In the case of high-rise elevators, the length of the rope between the car and the motor, as well as between the motor and the counterweight can often extend to a length of more than 250 meters. In 2016, alone, 32 high-rise buildings taller than 250 meters were constructed (2). Thus, the whole assembly acts similar to a giant spring, which makes it difficult to precisely control the deceleration and position of the car. Moreover, the ropes cause the car and counterweight to oscillate noticeably during, and specially at the end of the emergency stop event. Typically, additional rope can be added to stiffen the system. However, this increases mass, costs, and energy consumption of the system.

SG technology has progressed very slowly compared to other parts of the elevator. Although the mechanical nature of safety gears makes them very reliable, it also makes them virtually impossible to actively adjust for different scenarios.

1.2 Thesis Aim

Various solutions to the problem of uncontrolled deceleration have been disclosed in patents over the last two decades (see Section 2.4.3). However, none of these solutions have been commercially implemented due to international regulations and codes restricting actively controlled safety gears. Moreover, because of the general nature of patents, it is not known to what extent these patents may have been further developed or have shown promising results.

Therefore, the aim of this thesis is to model a small-scale free-falling elevator for an intelligent safety gear system in high-rise elevators. For this purpose, a physical test rig is created to validate the computer model. The validity of the test rig is verified with KONE test results. The proposed SG system will control the deceleration of the car by analyzing various variables of the elevator system and actuating a brake independent of the elevator ropes, thereby increasing the safety and comfort of emergency stops and making control of the car in the elevator shaft more predictable.

The system will be designed and made with data from computer simulations, small-scale prototype tests, and full-scale tests of existing components, as shown below in Figure 1.1. First, a simplified computer model will be developed to simulate the elevator car in an emergency using values and situations supplied by the Finnish elevator company KONE. The model will be simulated in MATLAB Simulink with a PID feedback loop and an oscillating mass simulating the ropes. Second, to validate the model, a scale prototype will be constructed that measures different variables under real conditions with real components. The physical prototype will test the algorithm for free-fall situations, the effect of oscillating mass simulating the ropes, and how the hardware reacts to external input. Third, these results will also be weighed against real-life measurements from KONE test facilities. Lastly, suggestions are given for next steps in research, development, and integration of the intelligent safety gear into commercial elevators.

This thesis will demonstrate the first steps for the development of an intelligent safety gear system according to Ulrich and Eppinger's Product Development Process (3) (Figure 1.2). The development of the end product can be categorized in three main categories: small-scale, full-scale, and commercial development (Figure 1.3). This thesis will develop the concept and test it in small-scale.
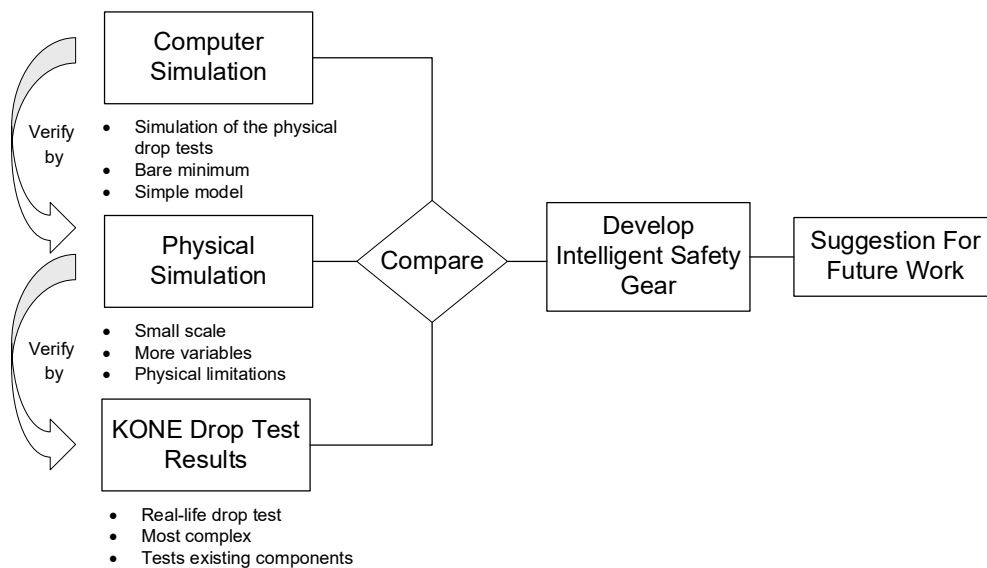
Figure 1.1 Thesis process map
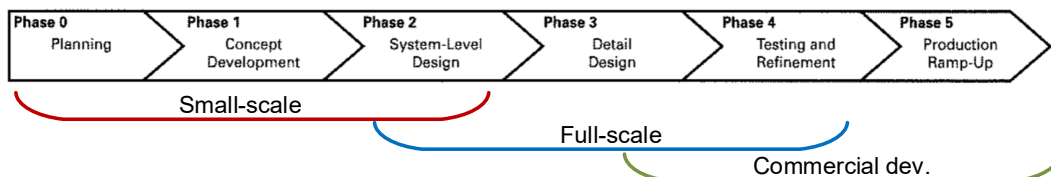
Figure 1.2 Ulrich and Eppinger's Product Development Process

3
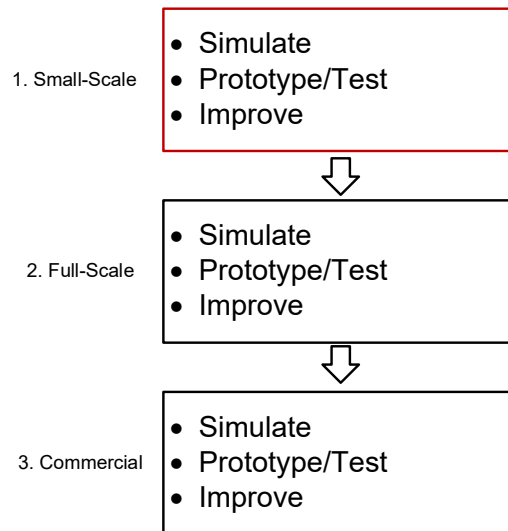
Figure 1.3 Development process

1.3 Scope of the Thesis

The thesis will be limited to high-rise elevators and the progressive wedge-type safety gears. The control system design will utilize only a PID feedback loop method and the performance of the control system. In addition, a safety analysis of the solution will be provided.

1.4 Thesis Structure

The remainder of this thesis is divided into 5 chapters. Chapter 2 will briefly cover the main components of an elevator system and state-of-the-art safety gears. Chapter 3 will describe the design and development of the system and the test setups. Chapter 4 will present and discuss the results from the different simulations and tests, as well as compare them to each other and known values, discuss safety, and make suggestions for future work. In Chapter 5 concluding remarks will be made.

CHAPTER 2

2 Commercial Elevator Systems

Safety is a critical factor in Elevator systems. Therefore, this chapter describes the basic components of modern elevators with a focus on state-of-the-art safety gear devices.

Elevators can be divided into four main subsystems: the elevator shaft, hoisting equipment, sling and car assembly, and safety equipment. These subsystems will be presented in Sections 2.1-2.4.

2.1 Elevator Shaft Components

This section presents the main components used for hoisting and arresting the elevator car, as well as briefly describes their functions. As shown in Figure 2.1, the elevator shaft [2] is the total volume in the building housing the travelling elevator and the majority of hoisting components. The shaft includes landings [3] and the pit [4] area. Located at the top of the shaft is the machine room [1], where the hoisting machine [5] (AKA motor), electrical cabinets and controls, and overspeed governors [14] are located. At the very bottom of the shaft is the pit where more components necessary to the function of the elevator (compensator, buffer (Figure 2.4) are placed.

Figure 2.1 KONE elevator components (KONE elevator company training material)

2.2 Hoisting Equipment

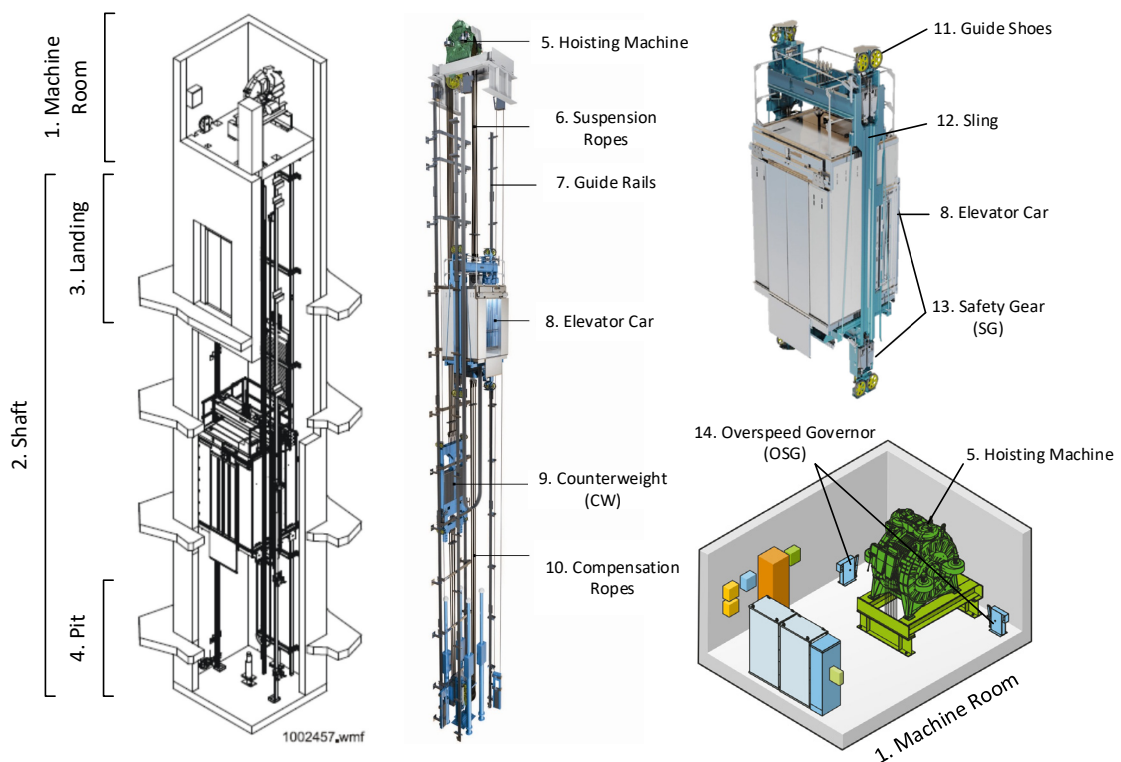The main hoisting components are the hoisting machine, suspension ropes [6], guide rails [7], counterweight (CW) [9], and the compensation ropes [10]. The hoisting machine or the motor, is an electric motor that translates the elevator car [8] and counter weight (CW) up and down in the shaft by transferring the energy through the suspension ropes. The motor also brakes and stops the moving car and counterweight. Suspension Ropes connect to and bear the weight of the car and the counterweight over the traction sheave (Figure 2.2), are rigid enough to reduce car movement during loading/unloading (4), and to transfer the energy from the motor to translate the car and the counterweight in the shaft. Guide Rails are metal T-shaped rails (Figure 2.3) meant to guide the car and the counterweight in the shaft and bear the safety gear tripping force. The guide rails extend for the whole length of the shaft. Counterweight (CW) is a moving mass connected to the car via the suspension ropes and compensation ropes to create traction between the sheave and the suspension ropes and to save energy by balancing the car. The counterweight weighs more than the empty car. Compensation Ropes are the ropes connecting the car to the CW from the bottom around a pulley in the pit. The compensation ropes help to balance the load during motion (torque balance), aid in traction, and save power.

2.3 Sling and Car Assembly

The major components of the sling and car assembly that are important to know in this thesis are the sling [12], elevator car, and the guide shoes [11]. The sling is a frame that supports the car (turquois color in Figure 2.1), absorbs shocks, balances uneven loads, connects the suspension and compensation ropes and carries external loads from buffers, Safety Gear (SG) [13], and such. The elevator car is an enclosed place to carry passengers and/or cargo with control buttons to control elevator. The car has damping to reduce vibrations. Hoisting and stopping components do not get attached to the car directly. In this work car, elevator, and sling may be used interchangeably. And finally Guide Shoes are roller guides with suspension that allow the sling to ride on the guide rails. These roller guides absorb some of the side to side motion of the sling and car during ride.
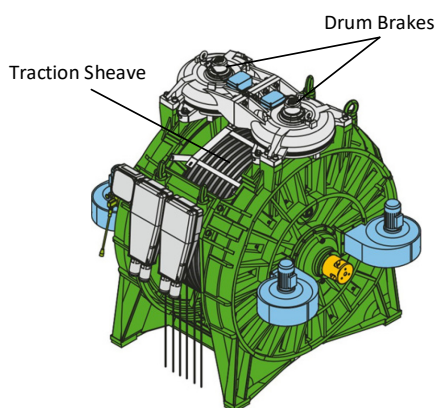

Figure 2.2: Motor and traction sheave. (KONE training material)

Figure 2.3: Elevator Guide Rail (http://www.ossosco.com)

2.4 Safety Equipment

Some of the safety equipment are the Safety Gear and the Overspeed Governor that are connected to each other and ensure the safety of the car in case of an emergency. The Safety Gear (SG) is an emergency equipment mounted on the top, bottom, or top and bottom of the sling. The safety gear is a purely mechanical device that gets triggered by the overspeed governor (OSG), engages the guide rails and brings the elevator to a halt in case of overspeed, suspension loss, or break in the safety chain. In this thesis wedge type safety gears are considered, since they are typically used in high-rise elevators. More about the function of the wedge type safety gear can be read in the following section. OSG consists of a triggering system and a loop of rope to sense overspeed and transmit the emergency brake triggering force to the SG. The OSG does not control the retardation force.

2.4.1   Safety Chain and Braking

The safety electrical systems (switches and monitoring system) of the elevator are connected in a chain called the "Safety Chain" which when broken will cut off the power to stop the elevator by automatically engaging the brakes (5). All the safety features of an elevator are fail-safe, meaning they are kept open by electrical signal. If the power is cut the safety features will engage and stop the elevator. For example, some links in the safety chain are

- Door contact switches,
- Stop button in the car,
- Overspeed detection,
- …,

Once the chain has been broken the drum brakes on the motor (Figure 2.2) are engaged to stop the elevator. This stops the moving car using the ropes. If the safety chain doesn't trigger or there is a fault in the system and the car is still accelerating, eventually triggering velocity will be reached and the OSG triggers the SG to bring the elevator to a halt. If all fails the last

line of defense are the buffers in the pit (Figure 2.4). Buffers are energy absorbing devices that act like bumpers absorbing the energy of the impact.
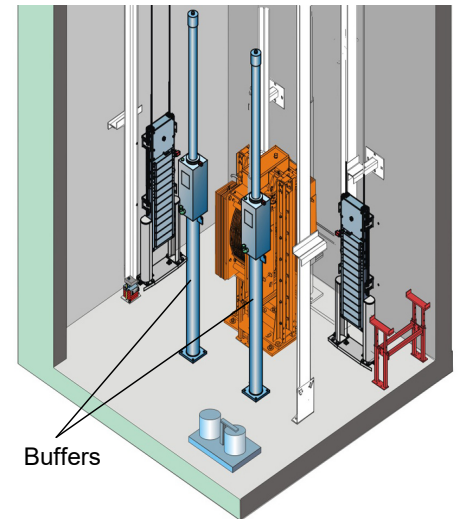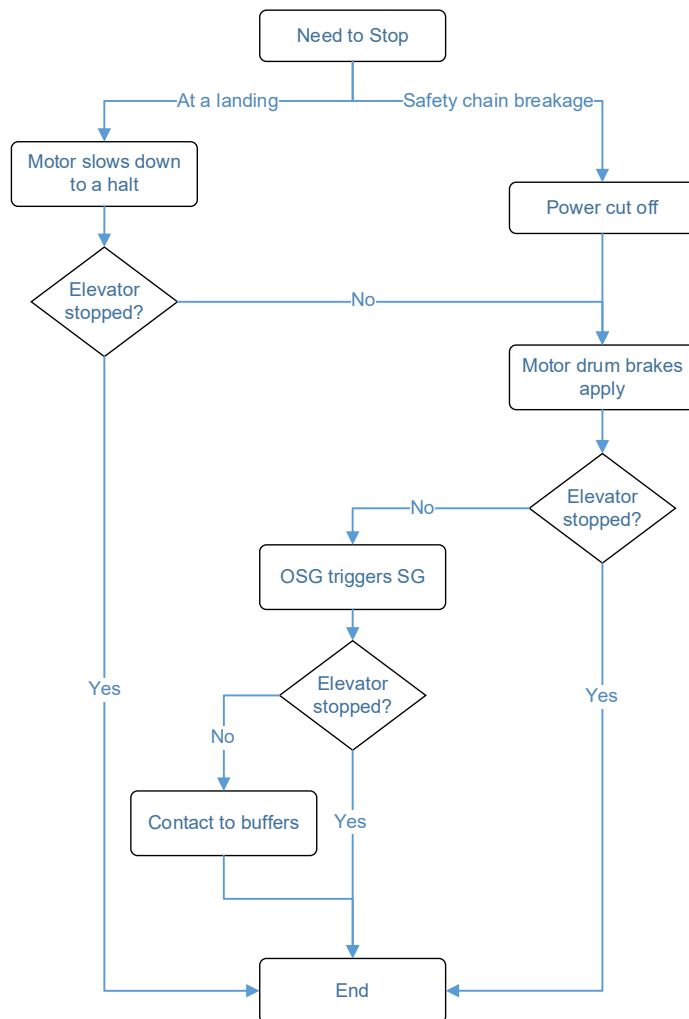
(KONE Hoisting Equipment (4))

Figure 2.4 Braking hierarchy and buffers

2.4.2   Safety Gears

In this section, different types of SGs will briefly be explained followed by the limitations of the progressive type.

SGs are conventionally divided into three main types (6): **Instantaneous**, **instantaneous with buffered effect**, and **progressive SGs** (Figure 2.5). **Instantaneous SGs** are the simplest type where the force is a function of and in direct relation to the distance travelled. After triggering, the braking force increases until the full stop of the elevator. This type is limited to speeds below 0.63 m/s. (1) **Instantaneous with buffered effect SG** is similar to the aforementioned, but benefits from the shock being absorbed by oil filled buffers. This type can travel as fast as 1 m/s (1).

Lastly, the **progressive SGs** are used for elevators travelling faster than 1 m/s (1). This type of SG holds a constant braking/friction force for the majority of the braking event. This type

of brake is adjustable for different cases such as car and CW size, condition of the rails, and travel velocity. The adjustments are done to keep the deceleration within the safe range, as designated by EN81-20:2014 (6). However, the adjustments can only be done manually by a professional and not dynamically in the OSGB 06/07 used by KONE (7).

Current OSGB 06/07 used by KONE in high-rise elevators are mechanical servos, meaning that they dynamically change the normal force to compensate for changes in coefficient of friction, leading to a constant friction force (7) (Figure 3.1). This makes the progressive SGs independent of velocity. However, the SG does not adjust the braking force depending on other conditions such as deceleration, location of the car in the shaft, and when oscillations from the ropes are induced. It is known that brake pad material exhibits a lower kinetic friction at higher speeds (8). The progressive SG can compensate for that by adjusting the friction force.
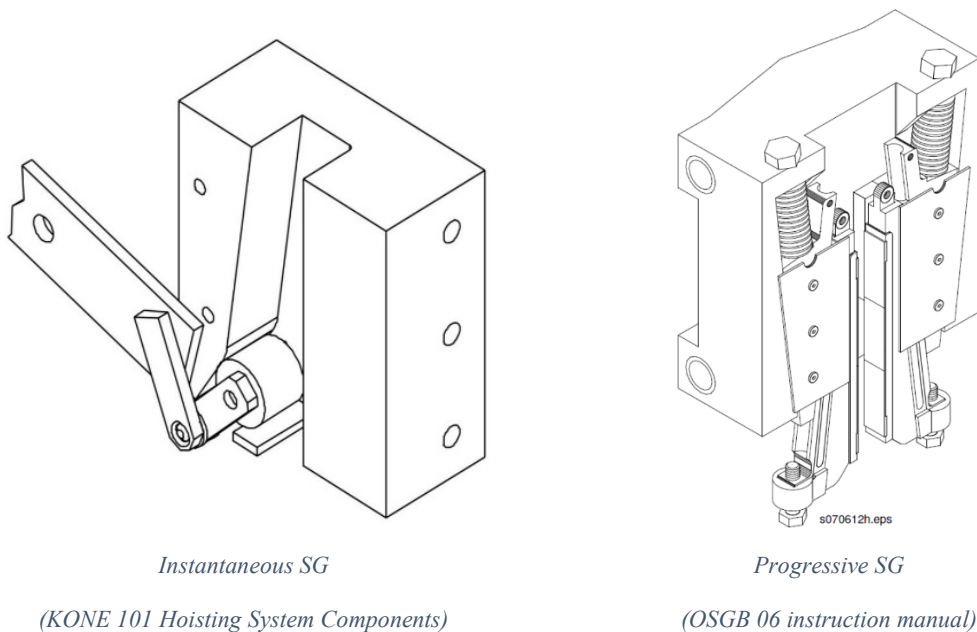

Instantaneous SG

(KONE 101 Hoisting System Components)

Progressive SG

(OSGB 06 instruction manual)

Figure 2.5 Two major types of SGs

All SGs are regulated by norms, such as EN81-20 (6), to be triggered mechanically via the overspeed governor. The OSG is connected to the safety gear via the safety rope with which it monitors the speed and triggers the SG if overspeed occurs. This limitation leaves the system vulnerable to cases where total suspension including the safety rope is lost or broken.

Application of SGs are limited to emergency cases where the motor emergency stop fails and the elevator must come to a halt. The application of SG is sudden, noticeable, and uncomfortable for the passengers. Once the SG is triggered it will bring the car to a stop regardless of where in the shaft it is. At this point the elevator is stuck in the shaft and needs human intervention (RDF: Recall Drive Feature) to reset it, move the car to a landing, and unload the passengers. After the activation of the SG the rails must be checked for damage (9). Often times, in the case of progressive brakes, the damage is only superficial and negligible. As can be seen in Figure 2.6 there is surface oxidation on the guide rails before the application of the SG. After the application, the rust is stripped and the shiny metal underneath is visible. Progressive SGs must be checked for the braking surface wear after 3-6 full speed, full load applications (7).

Rolling Area

Rusty Surface

Gripping Area

Shiny Surface
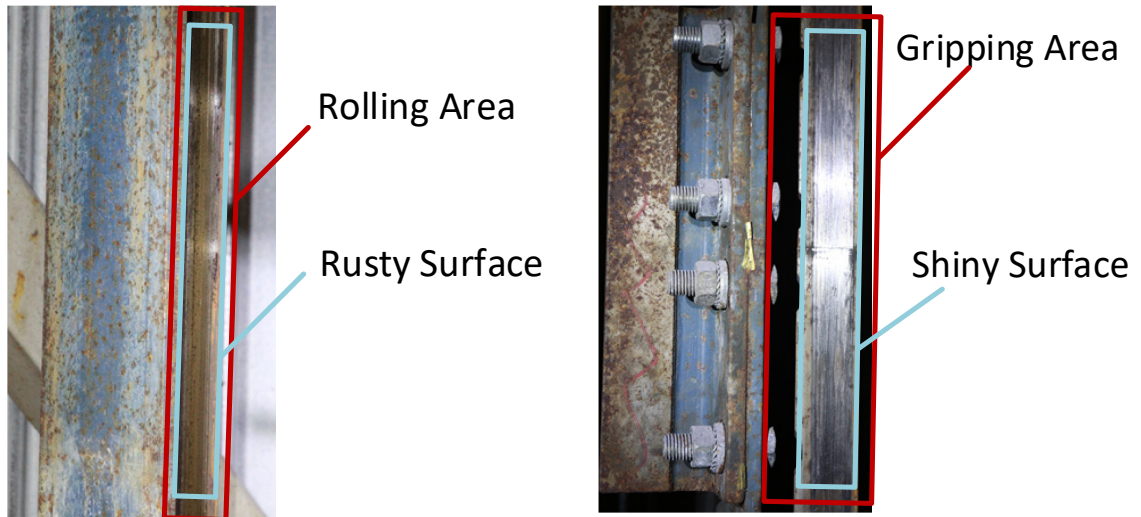
Rail 1) Before SG application with some rust.   *Rail 2) After SG application without rust.*

Figure 2.6 Rail tribology before and after progressive SG application. Images from KONE's Tytyri high-rise test facility, Lohja

2.4.3   Safety Gear Patents

In this section, a number of relevant patents are presented. Later on, in Section 5.2 there are used to suggest future work and draw conclusions.

Various Solutions in form of patents have been proposed for passive and active control of safety gears. These solutions include active self-contained hydraulic/electric brake actuators (Appendices 1, 2, and 3), sensing systems enabling actuation and control (Appendix 4), and mechanical servo type safety gears (Appendices 5 and 6).

Despite the solutions offered in these patents, safety regulations have prevented implementation of these patents in commercial elevators. Therefore, no evidence is available to verify their actual performance in a real-life setup.
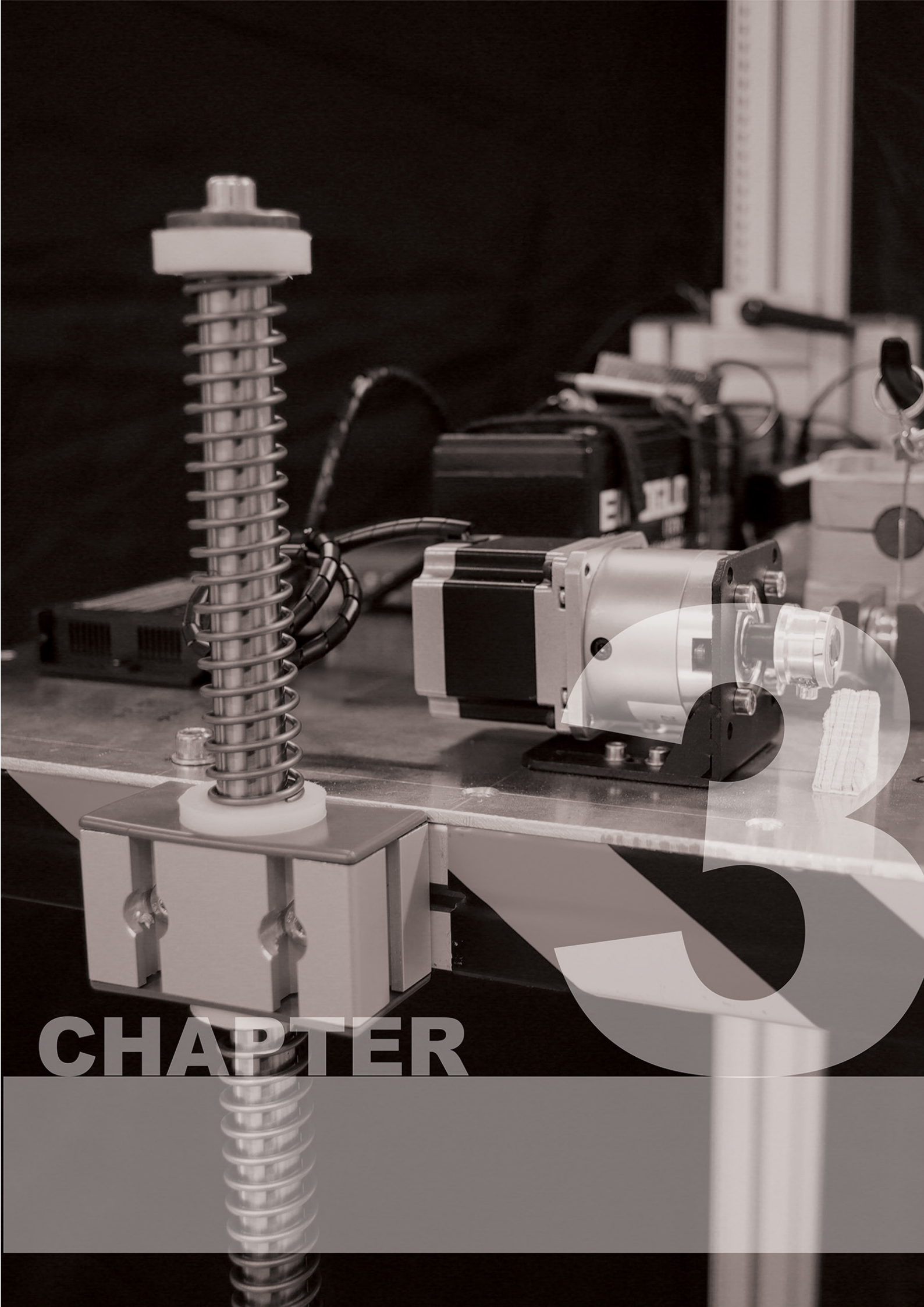
CHAPTER **3**

3 System Design and Development

As identified in the previous chapter, progressive safety gears (SGs) are currently limited by three major shortcomings:

- A lack of control,
- A purely mechanical system with a lack of intelligence,
- An uncomfortable and sudden event for passengers.

As a result, this thesis proposes the first steps in the development of an actively controlled safety gear system.

To accomplish this, a computer simulation of the falling elevator is constructed, and a physical model of an elevator is tested to collect empirical data for comparing the two simulation methods to each other. Finally, the two simulation methods are compared with actual test results from KONE's high-rise SG activation test.

3.1 Physics of a Decelerated Falling Object

In order to model the free-fall of an elevator car, it is first necessary to simplify the complex physics of this event. It is assumed that the elevator is in free-fall, there is no friction damping between the car and the surrounding, no drag induced from the atmosphere, and that the coefficient of friction is constant throughout the fall. Figure 3.1 shows the free body diagram of the forces applied to a free-falling mass on a rail.

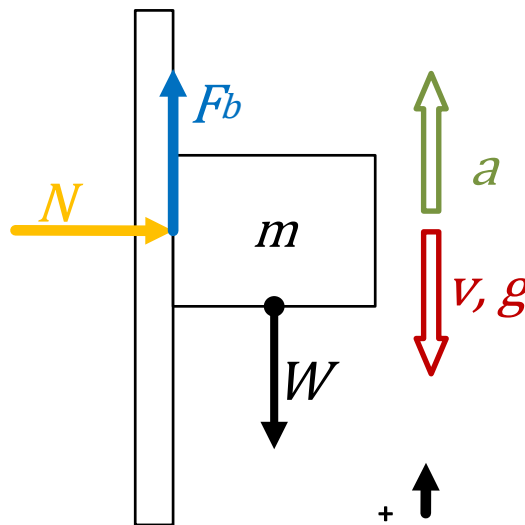*Figure 3.1 Free body diagram of forces*

In the case of a free-falling mass, the only force acting on the mass is the force of the weight accelerated by gravity. From Newton's first law where the force is the product of mass times acceleration, one can derive the following equation:

$$F = m.a$$

$$In\ equilibrium: \quad m.a - W = 0 \rightarrow m.a = W \xrightarrow{W=m.g} m.a = m.g \quad (1)$$

Where

F = force [N];
m= mass [kg];
W= weight [N];
g= gravitational acceleration [9.81 m/s²];
a = acceleration (downward)/deceleration (upward) [m/s²];

In the case of a free-falling elevator, the car will be sliding on the guide rails where the brakes will engage and apply a friction force, f_b [N], to stop the descending elevator. Therefore, it can be added to the equilibrium:

$$m.a + f_b = m.g \rightarrow f_b = m(g - a) \quad (2)$$

The friction force from the brake is the product of the coefficient of kinetic friction, μ_k, and the normal force, N [N], hereafter referred to as the gripping force.

$$f_b = N.\mu_k \rightarrow N.\mu_k = m(g - a) \rightarrow N = m\frac{g - a}{\mu_k} \quad (3)$$

From this equation, we can calculate the gripping force that needs to be generated by the brake. From the same equation, the deceleration can also be deduced as

$$a = g - \frac{\mu_k.N}{m} \quad (4)$$

Since the aim of the brake is to stop the elevator, the final velocity, v_f [m/s], must be zero; therefore, the velocity should be calculated as well:

$$v_f = v_i + a.t \quad (5)$$

Where
v_i = initial velocity [m/s];
t = time [s];
Plugging deceleration from equation # into the above equation yields velocity as a function of braking force:

$$v_f = v_i + \left(g - \frac{\mu_k.N}{m}\right).t \quad (6)$$

In the next section, these equations will be used to model the closed feedback loop computer model.

3.2 Design of a Closed Feedback Loop Computer Model

In this section, control system and feedback loops are briefly defined, followed by the design of the closed feedback loop computer model.

In order to control the accelerated fall of the elevator by means of brakes, it was necessary to use a control system. The current progressive SGs are controlled passively and mechanically by the OSG and elastic elements of the SG (i.e., spring washers (10)). The control system tested and developed in this thesis is an electronic control system. The system

is first modeled in MATLAB Simulink, and then a physical model constructed to test the software-hardware interaction.

According to Dorf & Bishop (11), a control system is "an interconnection of components forming a system configuration that will provide a desired system response." Furthermore, they define an open loop control system as a system that "utilizes an actuating device to control the process directly without using feedback." On the other hand, a closed loop feedback is a control system which "uses a measurement of the output and feedback of this signal to compare it with the desired output (reference or command)" In addition, the use of closed loop feedback enables rejection of external disturbances and improvement of measurement noise attenuation. (11)

Since current SGs are open loop controlled devices, it was necessary to integrate closed loop feedback in order to gain more control over the actuators using the input sensory data, thus allowing the settings to be actively changed. Thus, a closed loop control system is needed to control the deceleration of the elevator and compensate for external disturbances. By using the equations deduced in this section, a computer model was built in MATLAB Simulink, as shown in Figure 3.4.

For the controlled SG system proposed in this thesis, a simple Proportional, Integral, and Derivative (PID) controller was chosen (Figure 3.2). The PID controller is a three-term controller with a negative feedback loop that, once tuned properly, can bring the output to a desired steady state. The loop compares the output with the desired setpoint and multiplies the error by P, I, and D terms. PID controllers are widely used in industry. PID controllers are often used for position and state control applications, such as position control in Computer Numerical Control (CNC) machines, and furnace temperature control. Although popular, the controller is not without shortcomings. Limitations of the PID system include poor performance in large time delay, offsetting in ramp-type step response, and slow set-point tracking (12).
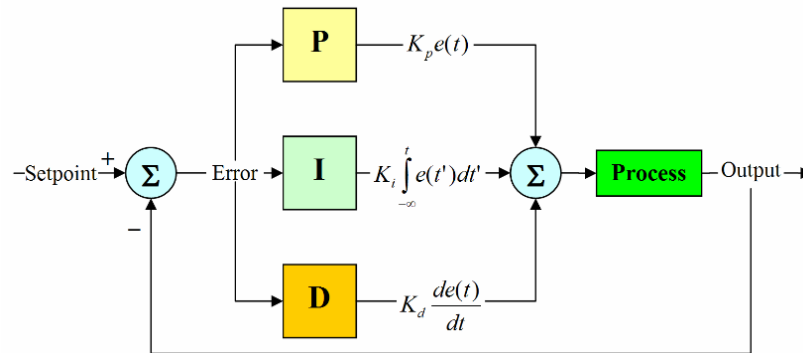

Figure 3.2 PID closed loop feedback (https://en.wikipedia.org/wiki/File:PID-feedback-loop-v1.png) (13)

3.3   Design of the MATLAB model

The MATLAB model (Figure 3.4) consists of five areas: the physical properties of the model [1], velocity loop [2], acceleration loop [3], oscillator sub-model [4], as well as the velocity and distance integrators [5].

Area 1: Physical properties of the model

The physical properties of the model [1] accelerate the mass (m) at the rate of gravitational acceleration. While the velocity is below the trigger threshold, the trigger blocks multiply the brake friction block by zero, which results in a zero-net braking force.

Area 2 & 3: Velocity and Control PID

Once the velocity reaches the pre-determined triggering velocity, the trigger blocks activate the velocity and acceleration loops [2 & 3] by switching the output from zero to the error value. The error value is calculated by subtracting the output velocity by the reference velocity zero. The reference velocity for the velocity loop is set to zero, since the brake has to fully stop the mass. Thereafter, the error generated is input into the PID block. The PID block multiplies the error by the proportional, integral, and derivative gains. The PID block is tuned to reduce the error value as fast as possible and without overshoot (Figure 3.3). The values of the PID were initially tuned using the automatic tuning feature in the software to obtain the "ball-park" values and then manually tuned further to achieve the desired response. Since the tuned values are not universal, cannot be generalized to other systems and are only valid for a range of velocities and masses, calculating the range was omitted from the scope of this thesis.
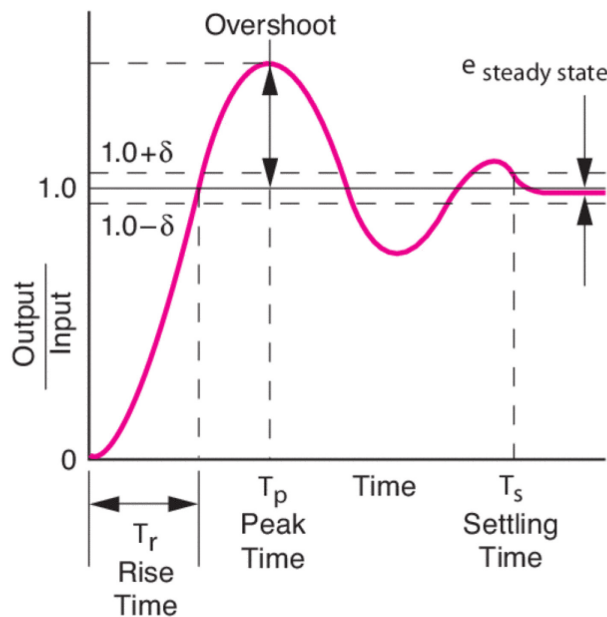

Figure 3.3 PID Overshoot (https://www.newport.com/n/control-theory-terminology)

16

Figure 3.4 MATLAB Simulink closed loop simulation

17

The trigger block simultaneously activates both the velocity and acceleration loops. The acceleration loop [3] calculates the error from the reference value of 0.6G (5.88 m/s^2), in compliance with the EN81 standard (6) as the safe deceleration value for emergency stop. The error is then input into the acceleration PID block. This PID was also tuned similarly to the velocity loop. The output of this block is then added to the output of the velocity loop, yielding the gripping force in Newtons.

Area 4: Oscillator

From Equation 4, it can be seen that the result of the gripping force multiplied by the kinetic coefficient of friction and then divided by the mass gives the friction-induced deceleration, which after being subtracted by the gravitational acceleration, results in the deceleration. In the next marked area [4], the deceleration is input as the exciting acceleration for the oscillating mass. The oscillator is a spring-mass system with a damper that simulates the oscillating ropes of the elevator. The accelerations of the mass are then output and summed with the deceleration to produce the total deceleration. The oscillator block is further explained in Section 3.3.1.

As the final step in the process, integration of the deceleration results in the velocity, and the second integration outputs the distance. The velocity and deceleration are then used as feedback to the velocity and acceleration loops, respectively. These outputs are then compared with the reference values and restart the feedback loop.
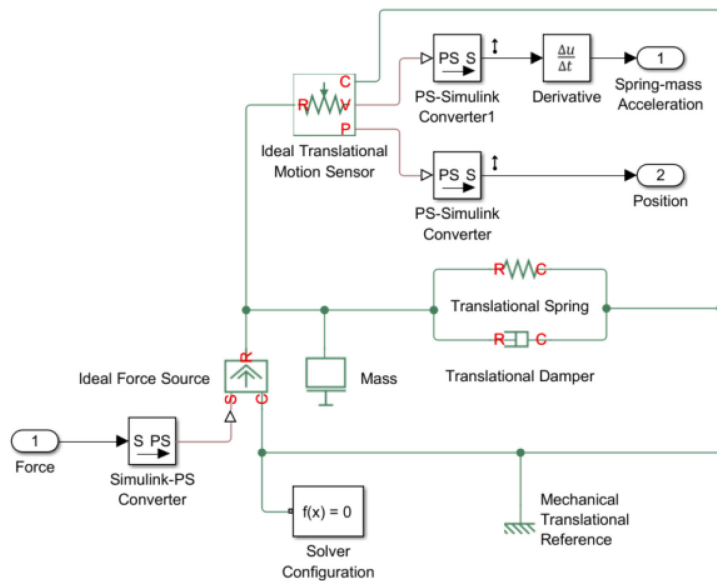

Figure 3.5 Oscillating mass inside of area 4, SimScape environment

The oscillator was modeled in SimScape, a modeling environment in MATLAB Simulink, which is suitable for modeling physical models. Since the environment is based on the flow of energy, the information entering and exiting the model must be converted. The green lines connecting the blocks represent the bidirectional flow of energy. The model must be grounded at some point to set a reference. In this model, a spring and a damper are connected in parallel. From one end, they are connected to the mass and from the other to the ground. The mass is excited by an ideal force source, for which the signal is externally input. The

reaction of the mass is measured by an Ideal Transitional Motion Sensor. The output has to be converted to Simulink signals before re-entering the Simulink work area.

The physical properties of this model were set to mimic the physical scale model (See Section 3.4).

Table 3.1 Values used in Simulink model. (ul: Unit-Less)

Parameter	Value	Unit	Parameter	Value	Unit
Mass	20	kg	Acceleration Kp	100	ul
Muk (μ_k)	0.3	ul	Acceleration Ki	50000	ul
g	9.81	m/s²	Acceleration Kd	-1	ul
Trigger velocity	2.0	m/s	Oscillating mass	1	kg
Velocity Kp	2000	ul	Spring 1 constant (stiff)	16'800	N/m
Velocity Ki	15000	ul	Spring 2 constant (soft)	1380	N/m
Velocity Kd	20	ul	Damper	1	N/(m/s)

3.3.1   Necessity of an oscillator

As mentioned earlier (Area 4: Oscillator), during the emergency brake event, the sudden stopping of the elevator causes the elevator ropes to oscillate. These oscillations are also transmitted to the car, causing discomfort for the passengers. Due to the constant braking force of current progressive SGs, they are not capable of dampening these induced vibrations. To simulate the effects of the ropes, an oscillator had to be added to the system. The oscillator consists of a mass-spring system. The spring was selected to vibrate the mass for about 3-4 periods and 10-12 periods of oscillation during the deceleration event, for when the car is at the bottom or close to the top of the shaft, respectively.[1] To simplify the model, only suspension rope vibrations were considered, as their vibrations are dominant among the vibrations from the compensation ropes due to their extra mass per length of rope (i.e., there are more suspension ropes than compensation ropes, hence a larger mass). Ropes on the CW side were disregarded, because their vibrations are dampened by the traction sheave and the compensation pulley.
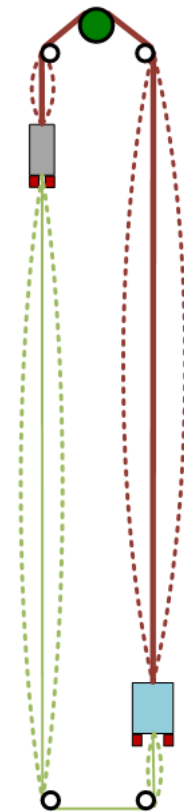
Figure 3.6 Rope oscillations

Figure 3.7 Free-body diagram of spring-mass system

The frequency at which the suspension ropes vibrate is dependent on the linear density, tension, and the length of those ropes. When the elevator car changes location in the shaft,

---

[1] According to empirical data by Jarkko Saloranta, dynamics expert at KONE

linear density and tension remain the same and the only variable is the length, which has an inverse relationship to the frequency of vibrations.

$$f = \frac{1}{2L}\sqrt{\frac{T}{\mu}} \quad (7)$$

Where:
    L: Length of rope [m];
    T: Rope tension [N];
    μ: Linear density of the rope [kg/m];

To calculate the stiffness of spring needed to oscillate a one-kilogram mass, the following equation was used:

$$\sqrt{\frac{k}{m}} = \frac{2\pi(n)}{t} \xrightarrow{\textit{While } m=1\ kg} k = (\frac{2\pi(n)}{t})^2 \quad (8)$$

Where
    k: Spring stiffness [N/m];
    n: Number of Periods [ul];
    t: Deceleration time [s];

After plugging in the known values (period, mass, and the event time), the two required spring stiffness values were obtained, as can be seen in Table 3.1.

3.4 Physical Test Rig

In addition to the computer simulation model, it was necessary to build a physical test rig for simulating the free-falling elevator. Therefore, this section describes the physical structure of the test rig, as well as data acquisition and processing equipment. The rig was used to test a brake controlled through closed loop feedback. In terms of its complexity, the test rig can be categorized somewhere between a computer simulation with low complexity/low fidelity and a full-scale high-rise elevator test with the highest complexity/highest fidelity. The test rig simulates the free-falling elevator by allowing a cantilever platform to slide down a rail with minimal friction under the gravitational pull without initial velocity. The platform is stopped via a hydraulic bicycle rim brake, which is actuated by a geared stepper motor. The brake acts on the surface of the aluminum profile skeleton (Section 3.4.1). The stepper motor is controlled by an onboard computer which senses the status of the platform using a linear encoder and an accelerometer. In the "pit" area of the test rig, a catch and bumper device is mounted to dampen the fall in case the brake fails to function properly. The collected data is transmitted to a computer for recording and analysis.

3.4.1   Mechanical Components and Properties

The mechanical components consist of an extruded aluminum skeleton, a linear slide, catch and bumper equipment, a hydraulic bicycle rim brake, and a geared stepper motor. Each of these will be discussed below.

Skeleton

The body and load bearing part of the test rig is constructed out of extruded 6063 aluminum sections (5 in Figure 3.9). Aluminum extrusions were chosen for their versatility, ease of use, construction rigidity, and ease of modification. The two main profiles used were 45mm × 45mm and 45mm × 90mm (Figure 3.8) in conjunction with various connecting components. It is possible to adjust the tilt of the rig using the five adjustable feet [8]. The platform [3] is able to move freely alongside the rail [1] via the slide [2] and allows for installation of various components on top of it. The installed components were comprised of a brake, stepper motor, stepper motor driver, sensors, computer, and batteries.

Profile 45 x 90 G

Profile 45 x 45 F

Part No. 20.1033/0

45mm × 45mm profile

Part No. 20.1015/0

45mm × 90mm profile
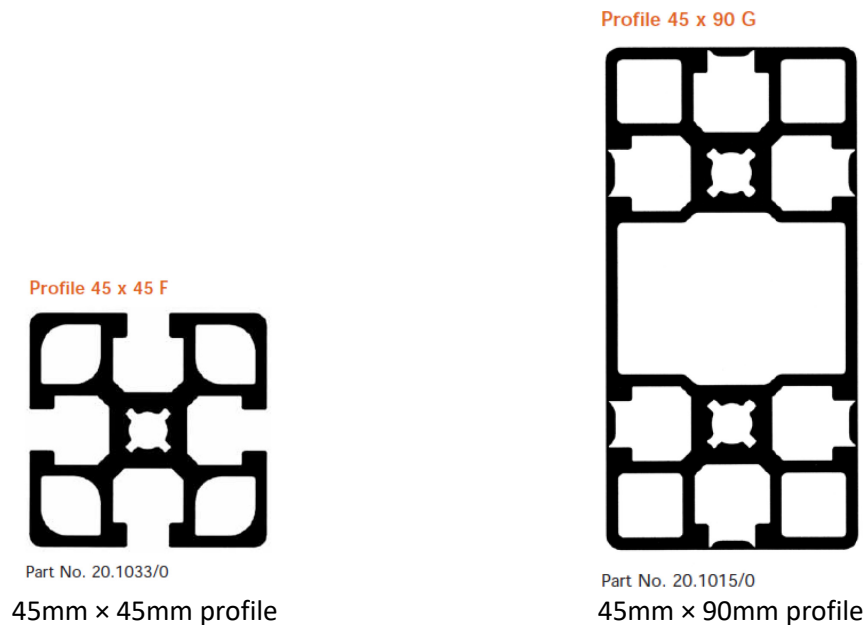
Figure 3.8 Aluminum extrusion profiles used. (Movetec Profiles)
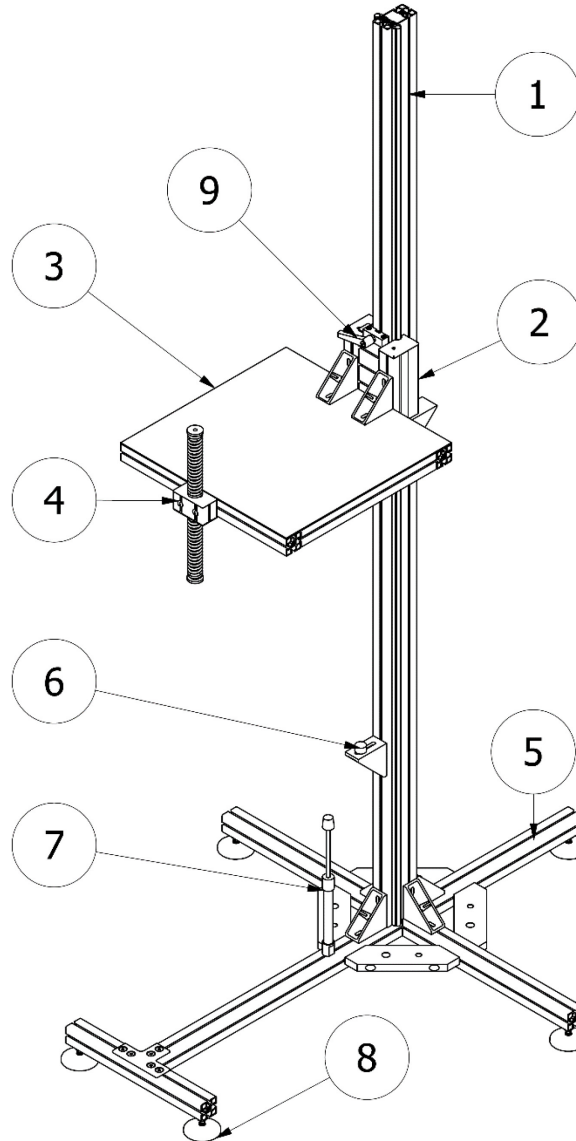
Figure 3.9 Mechanical construction of the test rig

Table 3.2 Test rig major components.

#	Component	#	Component
1	Rail	6	Catch device
2	Slide	7	Bumper
3	Platform	8	Adjustable feet
4	Oscillator	9	Manual brake
5	Aluminum extrusion		

The overall height of the rig is 2440mm ± 35mm with an effective travel length of 2265mm. The footprint of the rig measures 1335mm by 1045mm, and the dimensions of the platform are 500mm by 500mm. The fully loaded platform including the slide and minus the oscillator weighs 20kg.

Linear Slide

The linear rail and slides were chosen for this test rig, since they have a higher load carrying capability and accuracy (14), as well as lower friction and noise (15) than their recirculating ball bearing or plain bushing counterparts. The selected slide is able to carry 120 Nm of moment in the y-axis, which is the main loading mode of the platform. Two of the four bearings are mounted on offset screws, which enable adjustment of the bearing contacts and tightness on the rail. The slide is constructed of the same aluminum extrusions as the rest of the test rig, thus allowing more compatibility with fasteners and connecting parts.
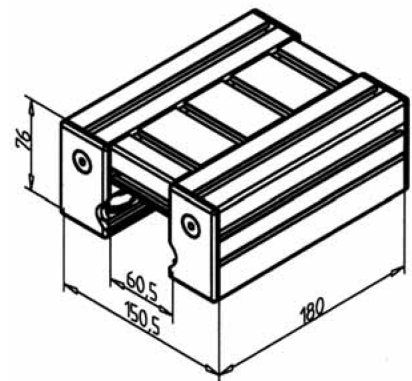
Figure 3.10 Slide LW 45 (Movetec Linear Systems)

The rail is composed of two ground hardened Ø12mm/Cf53 steel shafts mounted on an 45mm × 90mm aluminum profile.

Linear system Slides	**LR 12** Slide 45 4 bearings L = 180 mm
Mx max. My max. Mz max.	79 Nm 120 Nm 202 Nm
Fy max. Fz max.	3500 N 1500 N

Moment in y-axis   Manufacturer specified load bearing capabilities
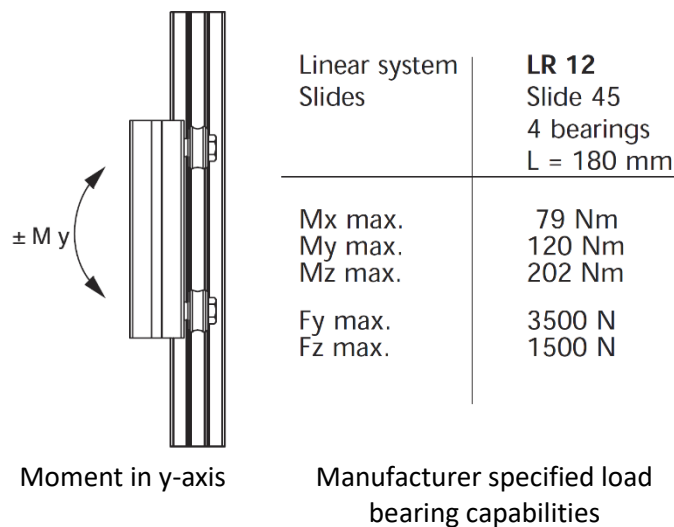
Figure 3.11 Slide LW 45 load bearing characteristics (Movetec Linear Systems)

Bumper and Catch Device

The bottom most part of the test rig is equipped with a bumper and catch device. The bumper [7] consists of a plugged pneumatic cylinder with a spring around the shaft (Figure 3.12). The bumper acts as a spring but does not dampen the energy of the impact, as opposed to oil-filled dampers. Before contacting the bumper, the platform meets the catch device (Figure 3.13). The catch device [6] is an angle bracket mounted on the rail. Mounted between the angle bracket and the rail is a low friction thermoplastic that allows energy dissipation through sliding friction. Once the platform contacts the angle bracket, the angle is allowed to slide on the rail surface, because the fasteners are tightened to a minimum torque (not measured, done by feel). The fasteners are tightened just enough to allow the bracket to hold the platform in place statically. The catch device was added later when, on one occasion, the platform did not stop and crashed into the bumper (Section 4.5). It was evident that the bumper alone was not sufficient to dissipate the energy of the impact.
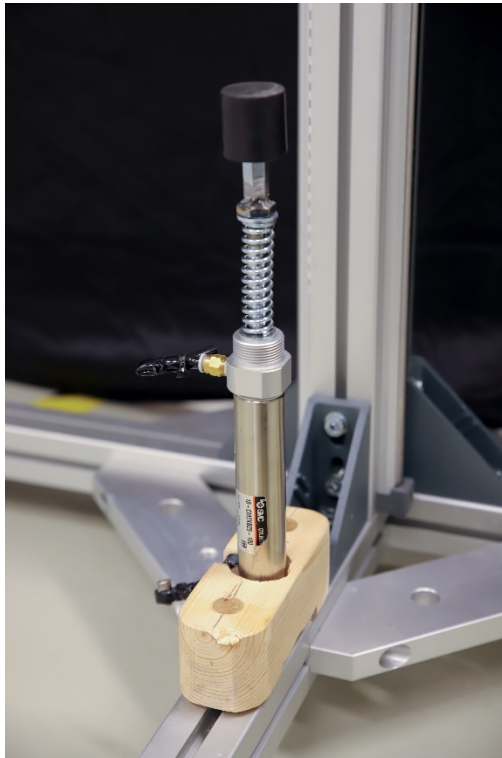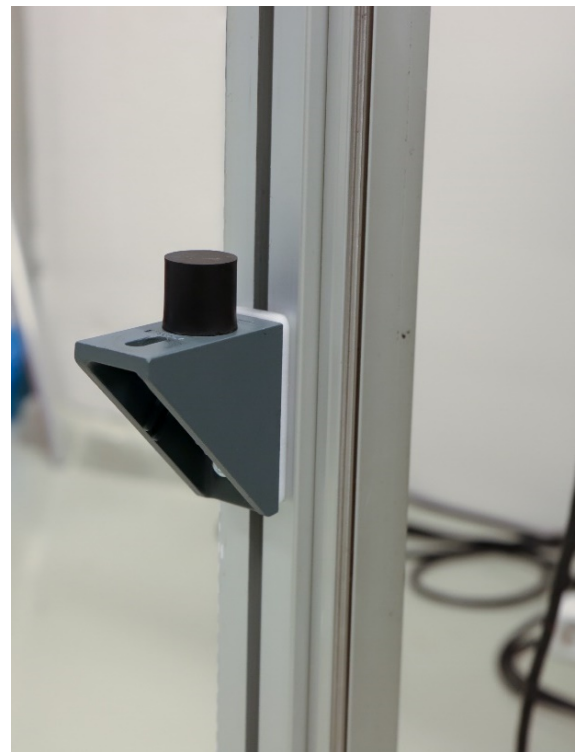
Figure 3.12 Bumper

Figure 3.13 Catch device

Oscillator

In Section "Area 4: Oscillator", a computer model of an oscillator was shown that served to simulate the oscillating ropes in the event of an emergency brake. The same phenomenon was tested in the physical test rig using a mechanical oscillator [8] in Figure 3.14. The mechanical oscillator, referred to as simply the oscillator hereinafter, is a one-kilogram shaft with compression springs on both ends around it, which is able to freely translate within a linear ball bearing, moving along the same direction as the platform. The oscillator is fastened to the platform with two M8 bolts. The bolts transfer the oscillation to and from the oscillator. As mentioned in Section 3.3.1 (*Necessity of an Oscillator*), the compression springs were sized to oscillate a one-kilogram mass within two ranges of frequencies: 6-8 Hz and 20-24 Hz.
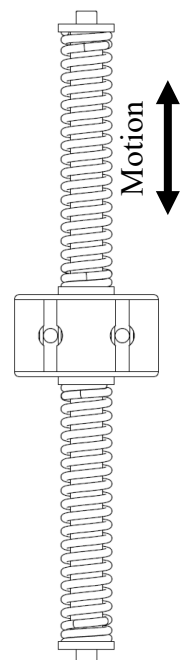
Figure 3.14
Oscillator front view

Hydraulic Bicycle Rim Brake
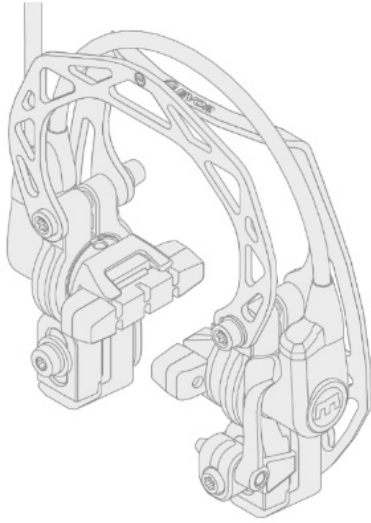
Figure 3.15 MAGURA HS 33 hydraulic rim brake (Owner's manual)

The motion of the platform was arrested using an off-the-shelf hydraulic bicycle rim brake. Hydraulic rim brakes are the better than cable actuated rim brakes, since each brake pad can be actuated independently, allowing them to be distanced from each other and customized fixtures to be utilized for attaching the brakes to the platform. Additionally, there is minimal backlash and flexion in the system, provided the hose system is free of air. The brakes were fixed to the platform using rigid aluminum L-brackets. The brakes actuate on the anodized aluminum surface of the rail (Figure 3.17). The pads are adjusted to have a clearance of about 1mm from the braking surface in the unactuated status. The brake pads are actuated by the brake handle, which was not modified to avoid damage to the braking mechanism. The brake handle is secured onto the platform, on which it is itself actuated by the geared stepper motor. The motor is connected through a spool and a pulley to the brake handle via a steel rope (Figure 3.16).

The coefficient of friction for the pads and the gripping force of the brake were not measured, since these properties were found to be unnecessary, as will be shown in the following chapters.
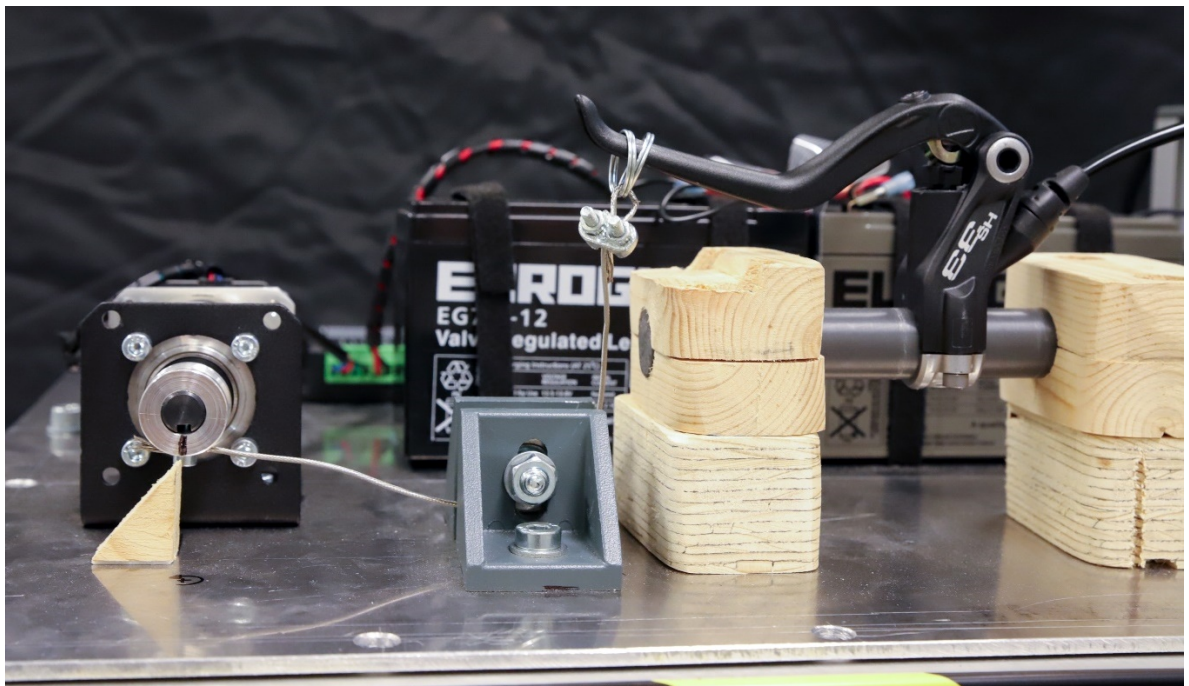
Figure 3.16 Actuation setup

Figure 3.17 Brake pad setup

Geared Stepper Motor

To actuate the aforementioned brake handle remotely on a moving platform, a suitable actuator is needed that is capable of moving the handle from the free to fully applied position (about 45mm) within 20ms at a force of 200N ± 30N (depending on the loaded mass on the platform). Although linear actuators are capable of exerting a large force and displace accurately, they would be too slow for this application. Similarly, solenoid actuators are quick but lack control and force (at least at an affordable price range). Hydraulic and pneumatic actuators need additional components (tanks, valves, tubing) to actuate, thus rendering them inadequate for a small moving platform. Consequently, it was decided to use a geared stepper motor. A stepper motor is an electric motor that has multiple windings and is able to take discrete steps, as well as holds a desired position. In some configurations, it is possible to add a gearbox to the output shaft to reduce/increase the rotational speed and torque. Stepper motors have a quick response, can take accurate steps, hold the position, and when coupled with a gearbox exert enough torque. The specified stepper motor is rated for 1260Nmm of torque without the gearbox. The torque generated by a force of 200N on a spool of 10mm radius equates to 2000Nmm. The specified 4.25:1 planetary gearbox with 90% efficiency increases the torque at the shaft to 5'355Nmm, thereby giving a safety margin of 2.68 for the specified motor. Table 3.3 displays the specifications of the stepper motor.

Figure 3.18: Geared stepper motor (https://www.omc-stepperonline.com/)

Table 3.3 Geared stepper motor specifications

Stepper Motor		Gearbox	
Step angle w/o gearbox	1.8	Gearbox type	Planetary
Holding torque w/o gearbox	1260Nmm	Gear ratio	4.25:1
Rated current	2.8 A	Axial load	100N
Inductance	2.5mH	Radial load	200N
Phase resistance	0.9Ω	Efficiency	90%
Type	Bipolar	Backlash (max)	1.5°

The rotational motion of the motor is translated into linear motion at the brake handle through a steel cable. The cable spools on a 20mm diameter aluminum spool around the shaft and is directed around a pulley to the handle. The pulley and the bike handle are adjustable, allowing the slack in the cable to be removed. The tension in the cable can be furthermore tuned by modifying parameters in the control algorithm.

The motor was paired with a DM542T stepping driver for control and power distribution.

3.4.2 Data Acquisition and Processing

For sensing motion and hence allowing actuation of the brake, appropriate sensors and processing power are needed. Therefore, this section describes the linear encoder, myRIO processor, onboard accelerometer, and finally the algorithm for enabling the processing of data.

Linear Encoder

In order to trigger the brake and ensure full arrest of the platform, it is important to determine the velocity. Since the velocity cannot be measured directly, it is necessary to derive the velocity of the platform from the displacement. Different methods for measuring displacement are available, including ultrasound, laser, and cable-extension transducer (Figure 3.20). However, an optical encoder was chosen because of its ability to measure the distance without any contact, complicated circuitry, inertia, hysteresis, and repeatability. The optical encoder made for this purpose has a resolution of 5mm. Even though it has comparatively lower resolution than similar commercial encoders, it is adequate for this application, with the added benefit of virtually costing nothing.

The encoder emits white light onto a black and white strip (Figure 3.21) attached to the side of the rail (Figure 3.22). The strip has 5 mm-thick successively alternating lines of black and white. The contrast of the light being reflected is measured by a photoresistor housed next to the light source but is separated in order to prevent unwanted light from shining on the photoresistor. The encoder housing (Figure 3.19) encloses the light source and the photoresistor and attaches them to the platform. The encoder photoresistor signal is digitized by NI myRIO and used with a Field Programmable Gate Array (FPGA) for real-time analysis.
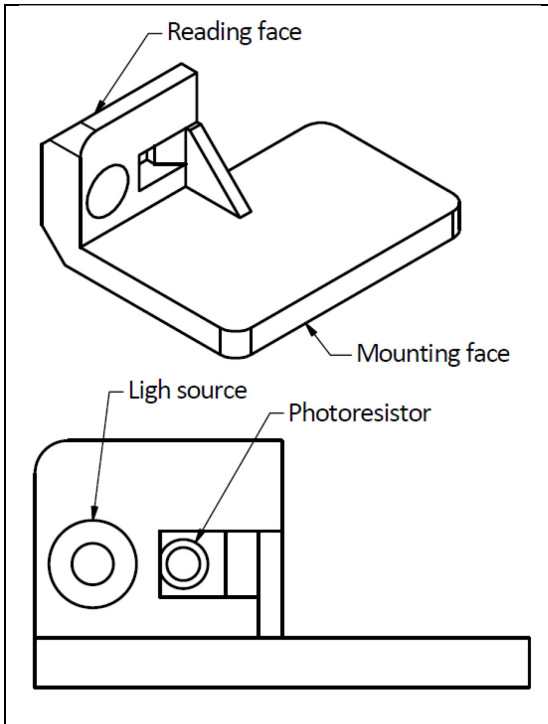
Figure 3.19 Linear encoder housing	*Figure 3.20: Cable-extension transducer. Due to the spring and the cable it has inertia which is not suitable for high acceleration applications. (http://www.autometer.com/string-potentiometer-12.html)*
Figure 3.21 Optical encoder with white light	*Figure 3.22 Encoder with successive strips*

myRIO and Accelerometer

myRIO (National Instruments, Inc.) provides reconfigurable Input/output (I/O) for prototyping. "It includes analog inputs, analog outputs, digital I/O lines, LEDs, a push button, an onboard accelerometer, a Xilinx FPGA (Field Programable Gate Array), and a dual-core ARM Cortex-A9 processor." (16) myRIO is programable with LabView (National Instruments, Inc.), which is a graphical block diagram programming environment for components produced by National Instruments, Inc. The powerful processor and FPGA allows quick remote computation for measuring and actuating. myRIO connects wirelessly via Wi-Fi to a remote computer station, thus eliminating the need for wires connecting to the moving platform. myRIO is equipped with a three-axis onboard accelerometer (Table 3.4 (17)). The onboard accelerometer will be utilized to measure the accelerations of the falling platform for subsequent use in control of the deceleration.

Table 3.4 Accelerometer specifications

Specifications	Values
Range	± 8 g
Resolution	12 bits
Sample rate	800 S/s
Noise	3.9 mg$_{rms}$ typical at 25°C

LabVIEW Program

LabVIEW is a system-design visual-based programming platform. LabVIEW programs are called Virtual Instruments (VIs), due to their resemblance to physical instruments. VIs consist of two programming platforms: front panel and block diagram. The front panel is the user interface of the VI. It includes scopes, buttons, gauges, and indicators. The block diagram is where the source code is visually programmed. It includes terminals, such as functions, constants, and loops. The front panel and block diagram are both interconnected, and each instrument in the front panel has a terminal in the block diagram. (18)

FPGAs are reprogrammable silicon chips that do not rely on separate applications to execute functions, such as computer processors, but rather the chip is rewired to execute a specific function. One can place FPGAs between computer processors and Application-Specific Integrated Circuit (ASIC). FPGAs have been described by National Instruments to have five benefits (19):

- *Faster I/O response times and specialized functionality*
- *Exceeding the computing power of digital signal processors*
- *Rapid prototyping and verification without the fabrication process of custom ASIC design*
- *Implementing custom functionality with the reliability of dedicated deterministic hardware*
- *Field-upgradable eliminating the expense of custom ASIC re-design and maintenance*

More importantly, FPGAs are deterministic (20). This means that once programmed, the user can be sure that each operation always takes exactly the same amount of time, which is

very important in closed loop feedback. Because of these benefits, myRIO FPGA was used in this thesis for the processing of the algorithm.

The control program consists of two individual programs: a program to manually actuate the stepper motor and one to run the velocity and acceleration control loops (similar to Simulink model in Section 3.3) The manual program (Figure 3.23) serves to adjust the initial starting point of the stepper motor shaft (Figure 3.24) and to restart the motor after each test run. This program allows the user to input the position of the shaft in terms of steps and the time interval between each of those steps, which determines the rotational velocity.
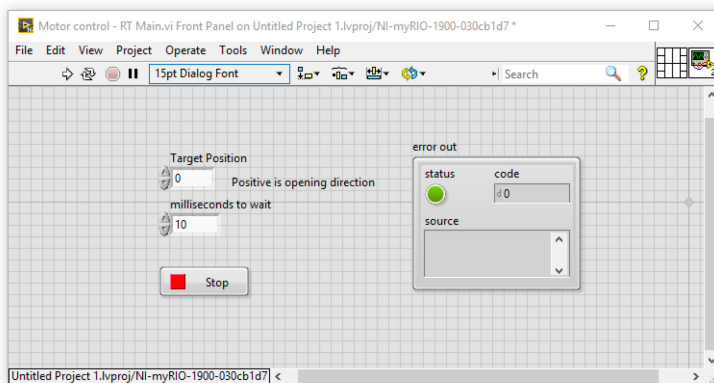
Figure 3.23 Manual motor control front panel   *Figure 3.24 Motor shaft initial position*
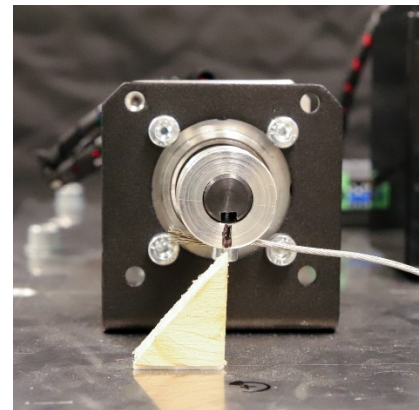
The velocity and acceleration control program is used to stop the moving platform with a set deceleration rate by reading the sensors and actuating the stepper motor. The program reads the relative position of the platform from the optical encoder, derives the velocity from the rate of change of position, and measures the acceleration from the accelerometer at the same time. Once overspeed is detected, it triggers the velocity and acceleration loops. The velocity loop reduces the velocity to zero by increasing the force on the brake, while the acceleration loop commands the motor to lessen the force in order to keep the deceleration at a set amount. The acceleration loop is disengaged after reaching a set velocity. This velocity represents 10% of the trigger velocity and is implemented to prevent the motor from disengaging the brakes after the velocity falls to zero. For faster travelling elevators, this velocity would be the velocity at which the friction characteristics of the pad change from kinetic to static friction.

The front panel of this program (Figure 3.25) allows for adjustment of many variables, including motor speed control, trigger velocity, acceleration set point, as well as velocity and acceleration PI loop multipliers. The adjustment of all these variables makes the test rig very flexible and adjustable for testing many scenarios.
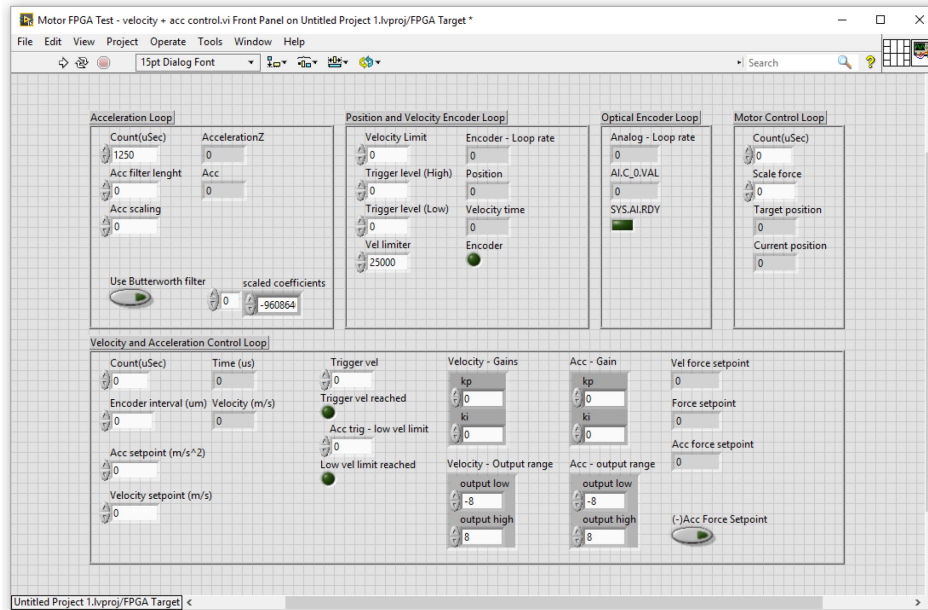
Figure 3.25 Velocity and acceleration control front panel

The platform control program used a PI loop feedback and did not use the derivative term (D term). The decision was made after realizing that the D term had little effect on the performance of the brake. The P and I terms in this program were manually tuned by trial and error.

3.5 Test Setups and Procedures

This section will describe the drop test at KONE Tytyri facility, and the testing procedure using the physical test rig.

KONE High-Rise Test

On October 24th 2017, KONE conducted full-speed safety gear drop tests for an double-decker elevator counterweight at the Tytyri test facility in Lohja, Finland. The test consisted of raising the counterweight to its maximum height, disabling the safety chain and the car safety gear, running the CW down the shaft to a maximum velocity of 10 m/s, and manually engaging the OSG to trigger the safety gear. Two consecutive tests were conducted. The control test is used as a reference for this thesis in Chapter 4. Table 3.5 lists the test specifications.

Table 3.5: KONE drop test specifications

Component	Spec.
CW mass	9,454 kg
Car mass	7,454 kg
Rope mass	2,455 kg
Trigger velocity	10 m/s

Testing Procedure

This section describes the test setup and testing procedure.

Initially, the check list below must be carried out before conducting the first test of the series:

1. Measure battery voltage. If the voltage is low, charge the batteries.
2. Ensure that all of the components are secured to the platform and that the wiring connections are well attached.
3. Test the balance of the platform. If shaky, adjust the feet and check for loose connections.
4. Check the distance between the bike brake pads and the slide. Check that the brake fluid has not leaked and that the brake is functional.
5. Make sure the bike brake hose loop is fastened and away from where the catch device would strike. (Figure 3.26)
6. Check the tension in the steel cable connecting the motor to the brake handle.
7. Test the location and sliding condition of the catch device.
8. Ensure that the bumper is functional.
9. Test the engagement of the manual brake and, when disengaged and falling, that the brake would not engage by itself.

Figure 3.26 Looped bike brake hose under the platform

Subsequent test consisted of the following steps:

1. Wear proper safety gear (i.e. helmet, eye protection, gloves)
2. Ensure that the motor and PI parameters are correct.
3. Ensure that the manual brake is engaged.
4. Reset the motor starting position (Figure 3.24)
5. Ensure that the transparent shields are in place (Figure 3.27)
6. Stand outside the taped area to the left of the platform. Grab the platform with one hand and release the manual brake with the other, making sure that your back is straight and knees are bent. At this point, the weight of the platform will be transferred onto you.

7. Lift the platform to the desired dropping height. Make sure no body part is in the path of the moving platform. Pay extra attention to your head and knees.
8. Run the control program. Wait for the green light (Figure 4.12) to turn on.
9. Once the green light is on, in a quick and swift motion, release the platform. A backward motion of the hands is recommended.
10. After the platform has fully stopped, engage the manual brake.
11. Stop the control program.
12. Save data results.

It is of utmost importance to have clear communication between the people conducting the test. Always double check Steps 2, 3, and 9. When using a 2 m/s trigger velocity and 0.6 G deceleration, the platform travels almost the complete effective length of the slide. For this reason, it is not recommended to test at a higher velocity (unless in conjunction with higher deceleration).

Transparent shields
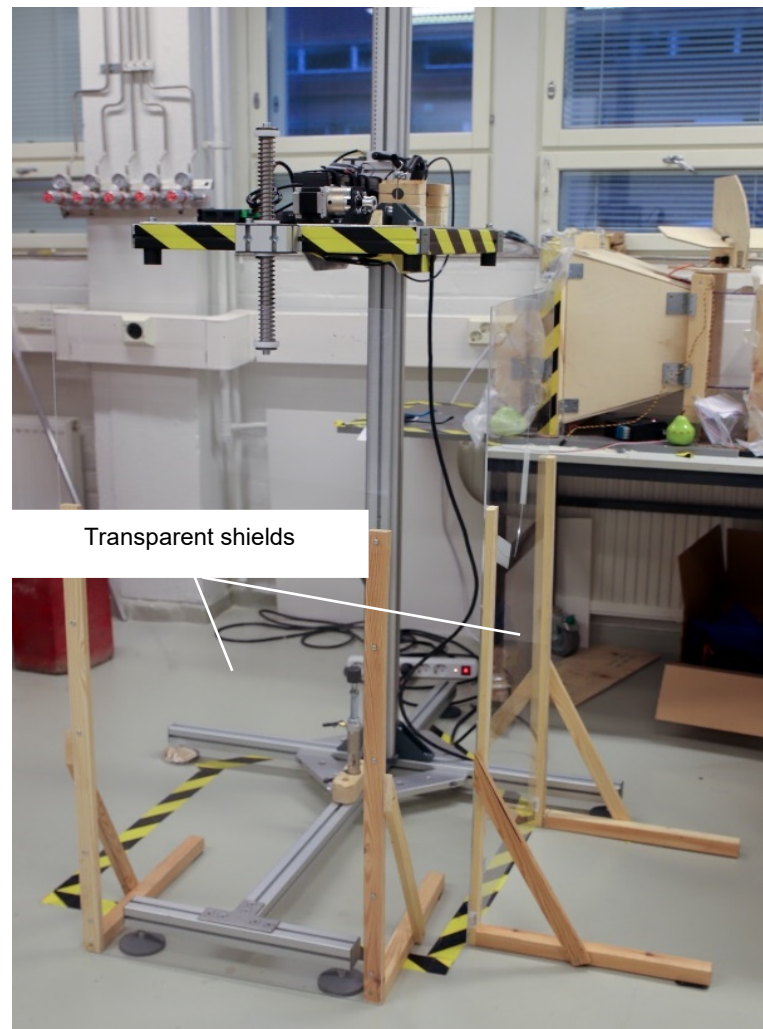
Figure 3.27: Test setup
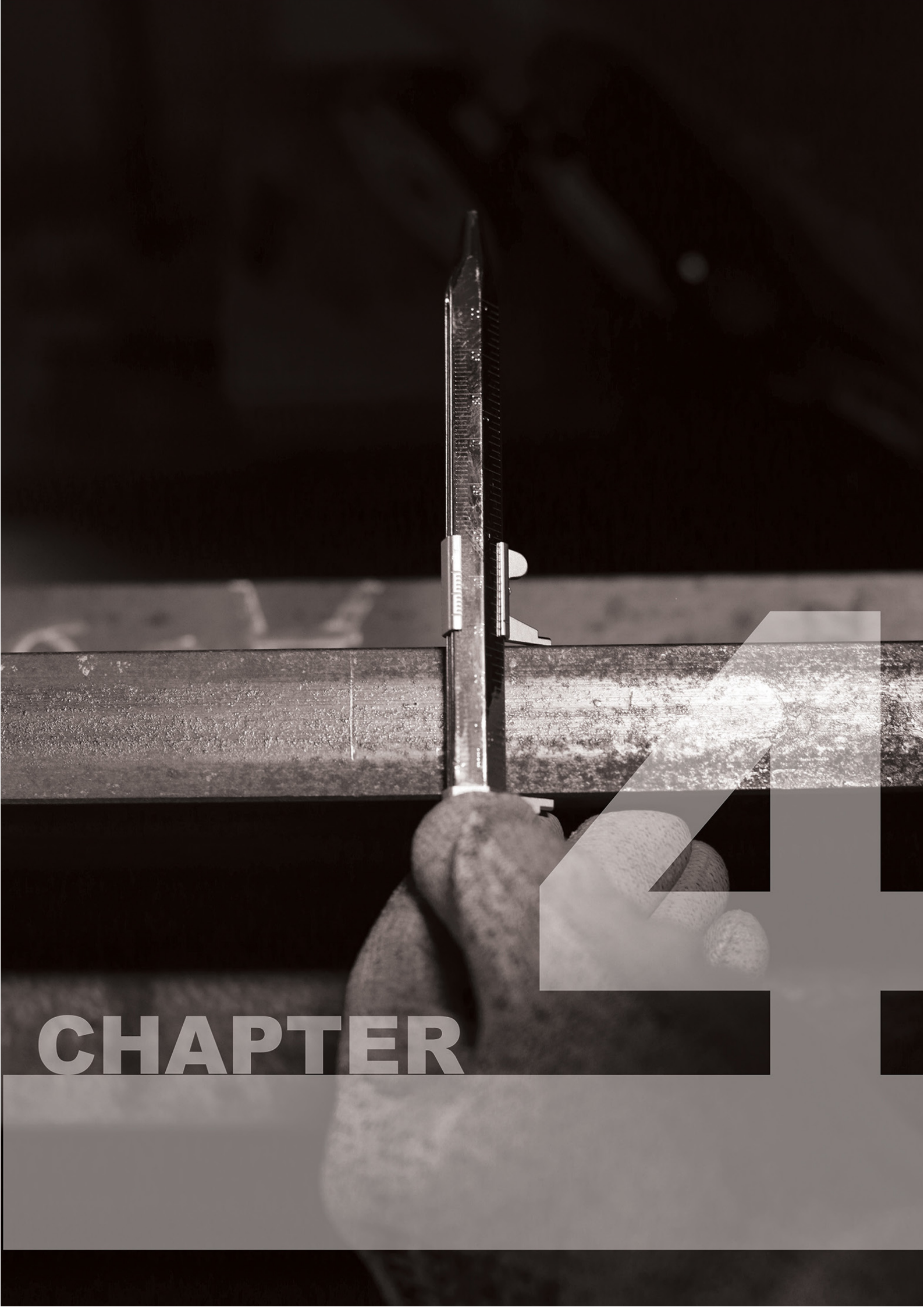
CHAPTER 4

4 Test Results

In this chapter, the results of the KONE Safety Gear Activation Test (SGAT), computer simulations, as well as physical test rig are presented and compared followed by analysis and discussion of the results.

4.1 KONE SGAT

As described in Section 3.5, two full-speed SGATs were conducted by KONE. In this thesis, the control test results will be used as reference data for verifying the validity of the results of the physical test rig. KONE's SGATs were conducted on the CW, which is sufficiently similar in its performance to that of the car as to be considered the same. The test was recorded by a multitude of instruments. The results of the tests are shown in Figure 4.1. Important to this thesis are the CW accelerations (blue), CW velocity (Red), distance travelled (yellow), and wedge location (green). Since there is no direct way to measure the force generated by the safety gear, wedge displacement has been commonly used, as it is the closest variable for describing the brake normal force (Figure 3.1)[2].
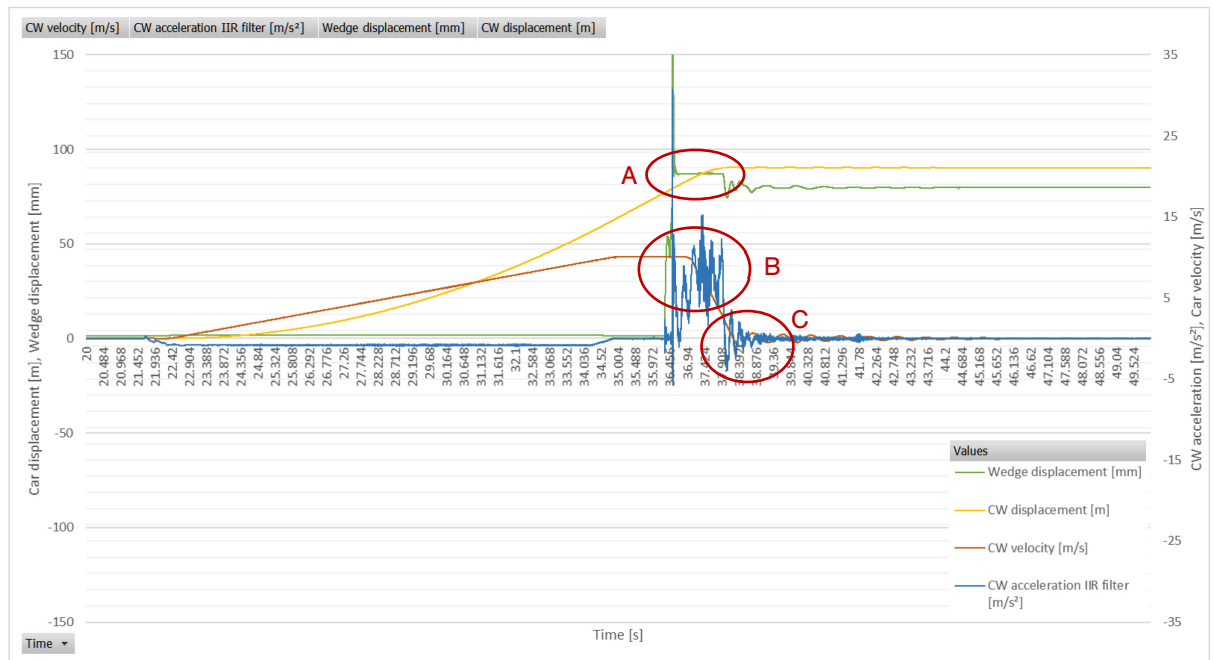
Figure 4.1: KONE Safety Gear Activation Test

The figure confirms that the safety gear applies a constant force during the deceleration [A], as shown by the wedge displacement (green line). The blue line demonstrates the acceleration of the counterweight. During deceleration [B], it can be seen that the vibrations fluctuate and hover around 5-10 m/s² (about 0.6-1G), which is considered in Norm EN81-20 (6) to be within the safe region, though the deceleration is not constant. As shown in the figure, the oscillations induced by the ropes attenuate after the braking event (C), which last for about two seconds.

---

[2] Personal communication, Jarkko Saloranta, KONE Dynamics Expert

4.2 Test Rig Verification

in order to evaluate the validity of the test rig results, the physical test rig was set up to exert constant force after overspeed detection in order to collect control data for comparison with KONE's SGAT. Since this test aimed to emulate KONE's SGAT, the oscillator with stiff springs (Section 3.4.1) was also integrated to simulate rope-induced oscillations. Figure 4.2 shows the constant force drop test results for the test rig.
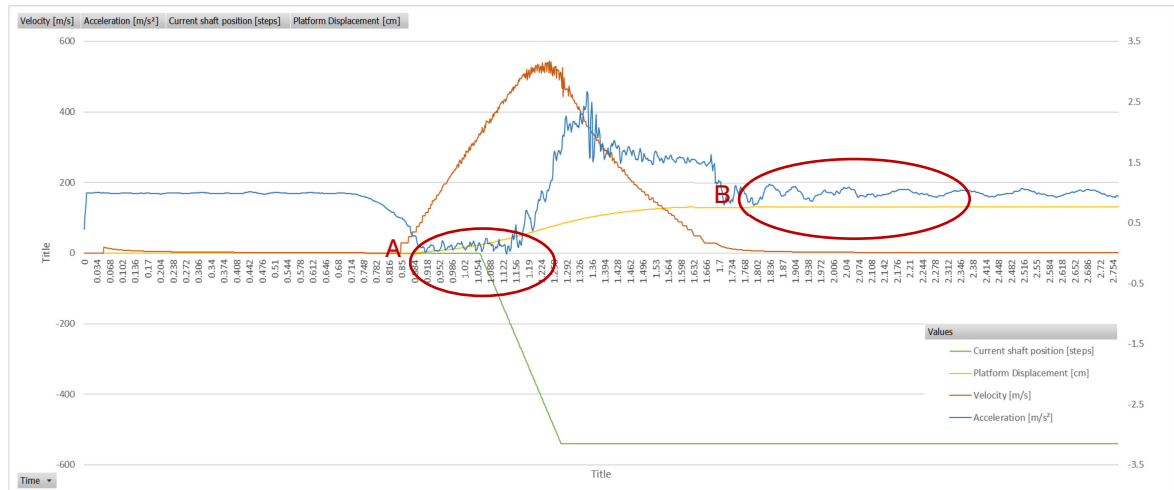
Figure 4.2: Constant force test rig drop

The green line shows the motor shaft position in terms of steps. As can be seen in Figure 4.2 the motor shows a step response (with a 270ms delay due to motor characteristics), which after triggering, moves to the maximum force position. The platform deceleration (blue line) descends and is, for the most part, without fluctuation. However, the average deceleration during the braking event was about 2Gs, the maximum value designated by EN 81-20:2014 (6). The oscillations induced by the oscillators can be seen during the free-fall period before the engagement of the brake [A]. However, soon thereafter, they are masked by the larger vibrations caused by the structure and the motor [B]. The same can be said for all subsequent tests. This demonstrated that the mechanical oscillator was not very effective for simulating rope oscillations. It is therefore suggested that the oscillator be modified if the same system is to be used in the future for tests and simulations.

This test was able to demonstrate that the tests conducted with the test rig, although not completely similar due to differences in size and components, exhibit the same major events as the real-life scenarios in order to be considered a viable test method: acceleration, overspeed detection, brake triggering, deceleration, full stop, and some oscillations.

4.3 Computer Simulation

The proposed safety gear control system was verified using the computer model explained in Section 3.3. The results of computer simulations for a free-falling mass with only the velocity loop engaged followed by the velocity loop and acceleration loop engaged are presented in the two following sections.

4.3.1   Simulation with the Velocity Loop Engaged

As mentioned in Section 3.3, the velocity loop serves to increase the braking force and reduce the velocity down to zero as rapidly as possible, whereas the acceleration loop works to reduce the braking force and keep the pre-set acceleration. Figure 4.3-Figure 4.5 show the simulated results for the engaged velocity loop.
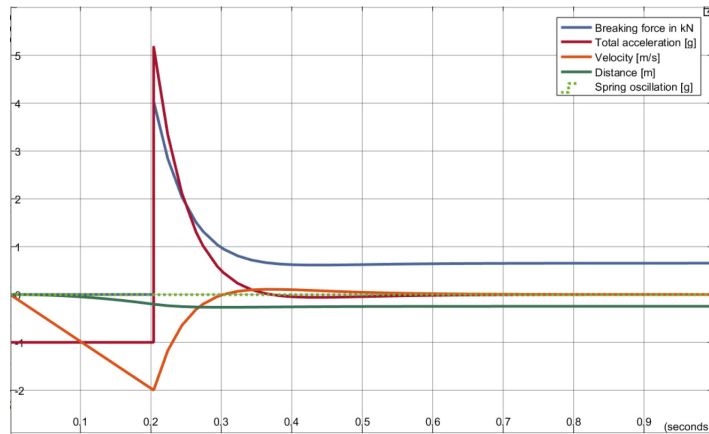
Figure 4.3 Velocity loop, no oscillator
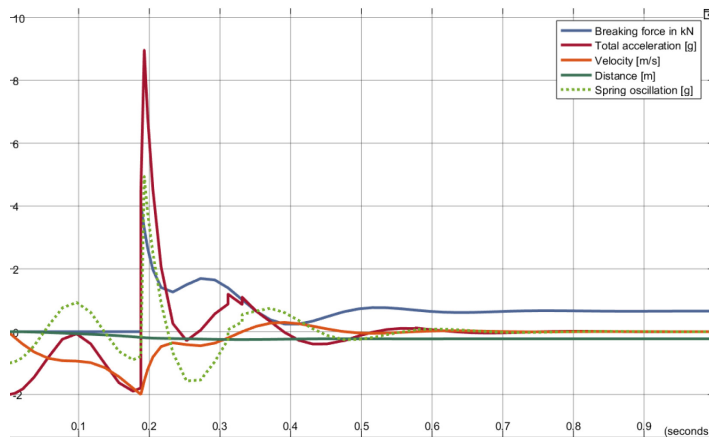
Figure 4.4 Velocity loop with soft spring oscillator
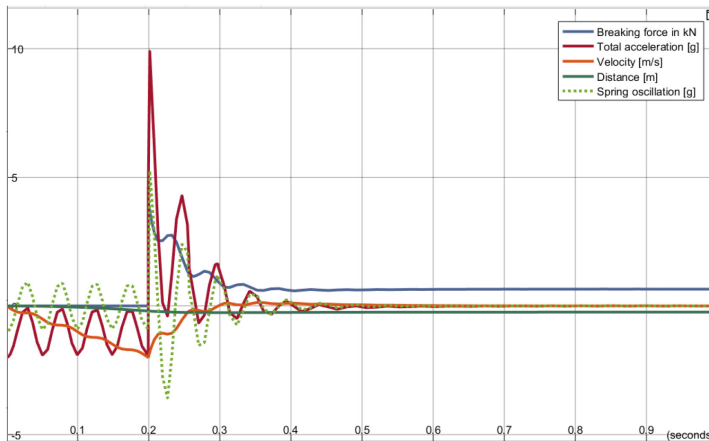
Figure 4.5 Velocity loop with stiff spring oscillator

Figure 4.3 shows the simulation results for the model without the oscillator. As soon as the overspeed is detected, the brake engages and brings the mass to a halt within 150ms; however, as expected, the acceleration is uncontrolled, exceeds the 1G limit, and reaches upward of 5G. In addition, since the force output is not limited, the result would be different from that obtained by the test rig with its physical limitations under the same conditions.

For the simulations shown in Figure 4.4 and Figure 4.5, soft and stiff spring oscillators (green dotted line) were added to the simulation. It can be seen from these figures that the force output responds somewhat to the external stimulus but is unable to completely counteract the stimulus. In these scenarios, the acceleration exceeds 8Gs and 10Gs, respectively. The parameter values used for the simulations can be seen in Table 3.1.

Comparing the results of Figures above clearly demonstrates that using a velocity loop alone is not a viable solution for controlled deceleration of a mass.

4.3.2 Simulation with Velocity and Acceleration Loops Engaged

Because using the velocity loop alone was demonstrated to be ineffective for controlled deceleration, it was clear that more control had to be added. Therefore, further free-falling mass simulations were conducted with both the velocity and acceleration loops engaged without (Figure 4.6) and with the oscillator (Figure 4.7 and 4.8).

Simulated next is the free-falling mass with velocity and acceleration loop engaged. As can be seen in Figure 4.6 and 4.7, the acceleration responses (red) are much smoother and closer to what could be expected for a controlled deceleration. From Figure 4.6, it is clearly seen that the acceleration loop maintains the acceleration at the predetermined 0.6G value. When the velocity is reduced to 0.2m/s (orange), the acceleration loop is disengaged and the velocity loop completely stops the mass.

In Figure 4.7 and 4.8, the soft and stiff spring oscillators were once again added to the simulation. It can be seen that when the acceleration loop is engaged, the motor adjusts the force to counteract the oscillations induced by the spring-mass system (green), resulting in a constant deceleration. This deceleration is only affected by the oscillator when the acceleration loop is again disengaged after reaching the lower trigger velocity. This is due to the lack of a "pull back" force on the brakes, while the velocity loop applies the brake. Therefore, the necessity of the acceleration loop is once more reiterated.

It is important to take into consideration that the results of the computer models shown in this section are idealized versions of the physical test rig with little complexity; i.e. the computer model does not include the motor response delay and motor inertia, nor any external sources of vibration and damping. Therefore, the model cannot predict the exact outcome.
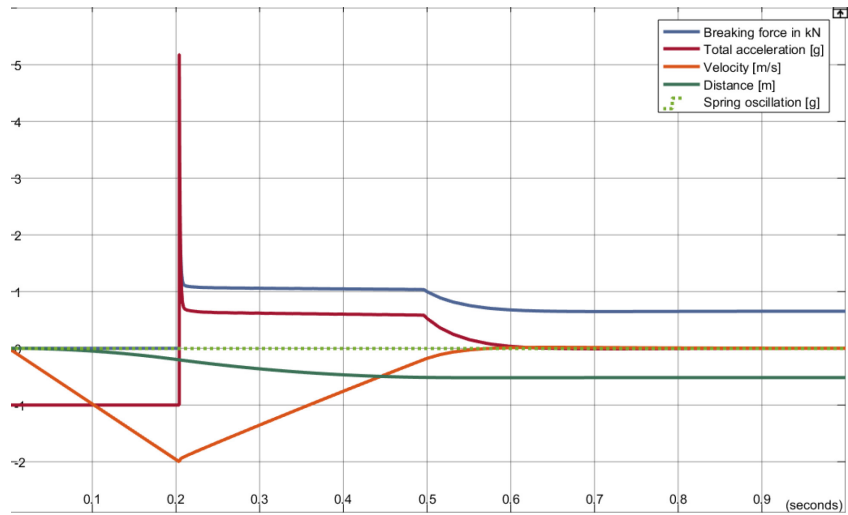
Figure 4.6 Velocity and acceleration loop engaged. No oscillator
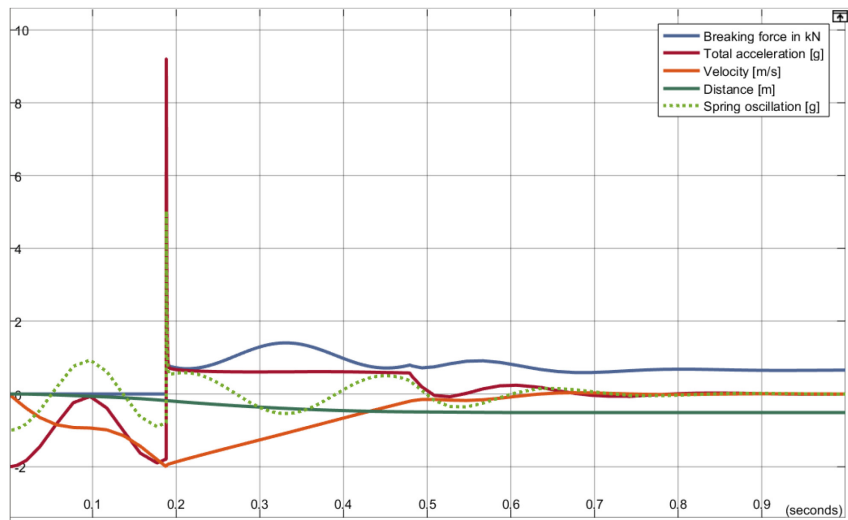
Figure 4.7 Velocity and acceleration loop engaged. With soft spring oscillator
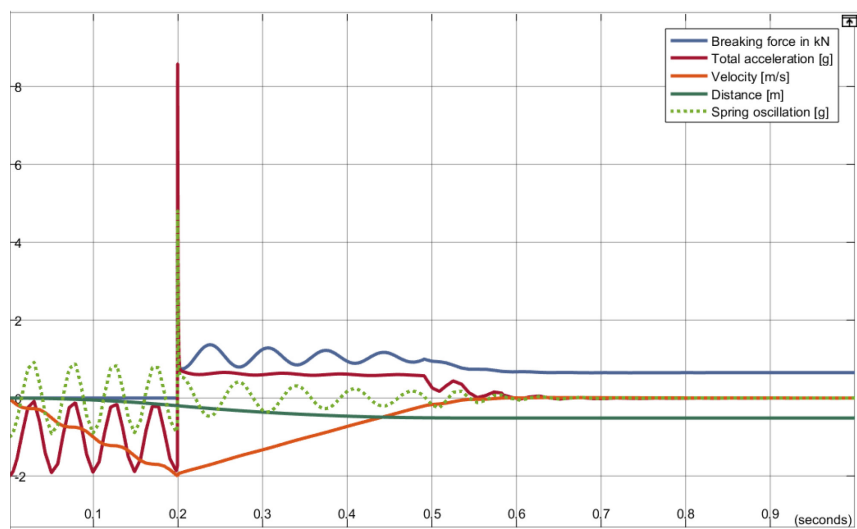
Figure 4.8 Velocity and acceleration loop engaged. With stiff spring oscillator

4.4 Physical Test Rig Results

In Section 4.2, it was established that the physical test rig is able to demonstrate the same major events as real elevators. Therefore, this section uses the physical test rig to verify the results of the computer simulation in a real-life environment.

Although ten different tests were conducted, only three will be shown in this section, because the oscillator (as explained in Section 4.2) had no significant effect on the vibrations. The three tests consisted of a drop test with the velocity loop engaged, drop test with the velocity and acceleration loops engaged, and finally Butterworth filtering. The rest of the test results are shown in Appendix 8: Physical Test Rig Results.

4.4.1 Drop Test with Velocity Loop Engaged

In this test, the acceleration loop was disabled and only the velocity loop was engaged. It might not be surprising to notice that this test is similar to the constant force test in Section 4.1: the motor had a step response to the velocity trigger [A] also the deceleration is descending and elevated at around 2Gs [B] (Figure 4.9). This demonstrates that using a velocity loop alone renders an effect similar to that of a constant force brake. The reason for this is that, as mentioned earlier and to reiterate, the velocity loop applies the brake, and the acceleration loop reduces the braking force to control the acceleration. Thus, the velocity and acceleration loops resemble "Yin and Yang": opposite in force but complementary in function. Table 4.1 shows the parameters used in the test.
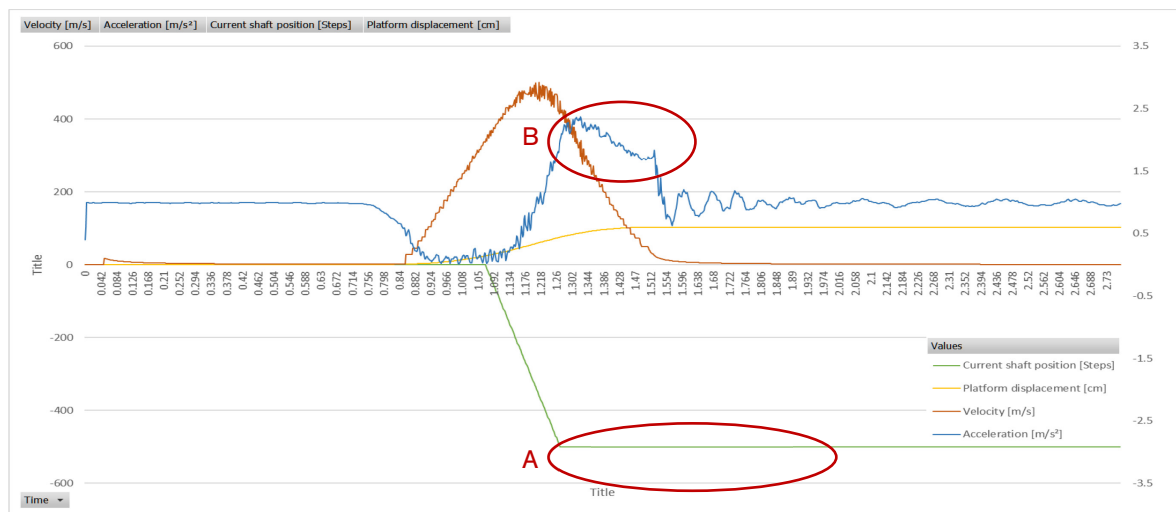
Figure 4.9 Velocity control test rig drop with stiff spring oscillator

Table 4.1 Velocity con. with stiff spring oscillator parameters.

Velocity	Value [ul]	Acceleration	Value [ul]	Motor	Value
Gain kp	7.00	Gain kp	0.00	Scale force	20.00
Gain ki	0.1	Gain ki	0.00	Motor loop	200.00 [µs]
Output range – low	-25.00	Output range – low	-20.00		
Output range – high	0.00	Output range – high	0.00		

4.4.2 Drop Test with Velocity and Acceleration Loops Engaged

In this test, both the acceleration and velocity loops were engaged. As can be seen in Figure 4.10, The addition of the acceleration loop caused the motor to exhibit a sawtooth response [A], as illustrated by the green line. This response is caused when the accelerometer senses that the acceleration is increasing and hence commands the motor to reduce the braking force in order to decrease the deceleration. This, in turn, causes the platform to decelerate too little, which the accelerometer senses and then commands the motor to increase the braking force. This back and forth between braking and releasing the brake causes vibrations [B]. The situation is worsened because of the inherent delay between the command sent and the actual actuation of the motor. Despite the sawtooth response of the deceleration [B], the deceleration averages about 0.6Gs.

If the motor delay had been lower and the tuning less aggressive, this would have minimized the sawtooth response. This would suggest that the PID parameters would need more fine tuning, which remain outside the scope of this thesis. The parameters used in the test are shown Table 4.2.
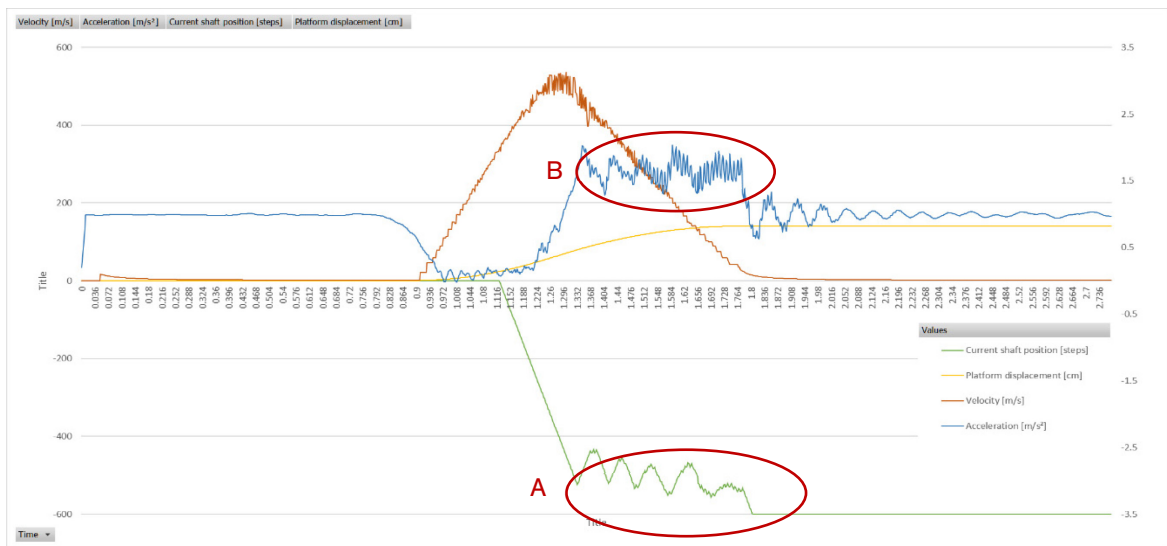
Figure 4.10 Acceleration and Velocity control test rig drop with stiff spring oscillator

Table 4.2 Acceleration and Velocity control test rig drop with stiff spring oscillator parameters

Velocity	*Value [ul]*	*Acceleration*	*Value [ul]*	*Motor*	*Value*
Gain kp	7.00	**Gain kp**	0.50	**Scale force**	20.00
Gain ki	0.1	**Gain ki**	0.00	**Motor loop**	200.00 [µs]
Output range – low	-30.00	**Output range – low**	-20.00		
Output range – high	0.00	**Output range – high**	0.00		

4.4.3   10 Hz Butterworth Filtering

According to ISO18738-1 (21), the acceleration measurement should be processed through a 10Hz low-pass 2-pole Butterworth filter. This norm was therefore used to conduct a test to see its viability for this test setup. However, the frequency was too low compared to the short time of event (~500ms) and the filter introduced too much lag into the acceleration measurement (Figure 4.11). Because the stiff spring oscillates between 20-24 Hz, which is already twice the filtering frequency, the frequency was increased to 45Hz in an attempt to capture the details of the vibrations while still maintaining a low-pass filter. As a result, a 5-point moving average filtering method was used for the remainder of the tests. Table 4.3 shows the parameters used in the test.
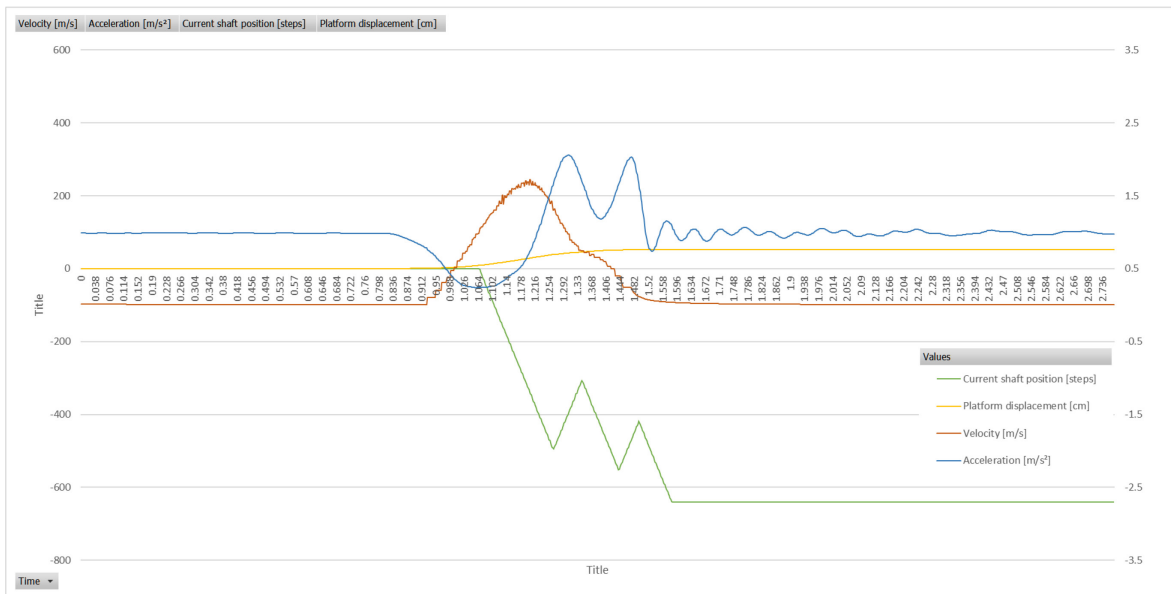
Figure 4.11 10Hz low-pass 2-pole Butter worth filtered results

Table 4.3 10Hz low-pass 2-pole Butter worth filtered results parameters

Velocity	Value [ul]	Acceleration	Value [ul]	Motor	Value
Gain kp	7.00	**Gain kp**	0.50	**Scale factor**	20.00
Gain ki	0.1	**Gain ki**	0.00	**Motor loop**	200.00 [μs]
Output range – low	-32.00	**Output range – low**	-20.00		
Output range – high	0.00	**Output range – high**	0.00		

Independence from Mass and Coefficient of Friction

The algorithm that controls the test rig is independent of the mass and coefficient of friction. The system is flexible to some degree for accommodating changes in the mass and friction coefficient owing to the nature of the closed loop feedback, i.e. the feedback loop will increase the force if the mass/friction is too high/low and vice versa.

4.5 Test Rig Failure Case

Upwards of 50 drop tests were conducted on the test rig at trigger velocities as high as 2.5m/s. The rig demonstrated near perfect performance with reliable stops. There was only one occasion when the brake did not trigger and the platform crashed into the bumper at the bottom of the travel. This crash was not due to component failure or algorithm error, but rather human error. The error occurred when the platform was raised to the top of the rig, the brake algorithm was not properly activated, and before the mistake could be noticed the platform was released. The crash caused damage to the test rig, but fortunately the damage was only to the non-essential components that were able to be fixed quickly (Figure 4.13). To prevent this error from happening again, a large green light (Figure 4.12)was added to the front panel of the control program that would indicate clearly when the program was running, as well as a clear test procedure was agreed upon (Section 3.5). In addition, because of the inadequate placement of the bumper, the slider slipped off the rails (Figure 4.14), causing some surface damage to the rails. To mitigate such damage in the future, the bumper was moved closer to the slide and the catch device (Section 3.4.1) was added to the rig.
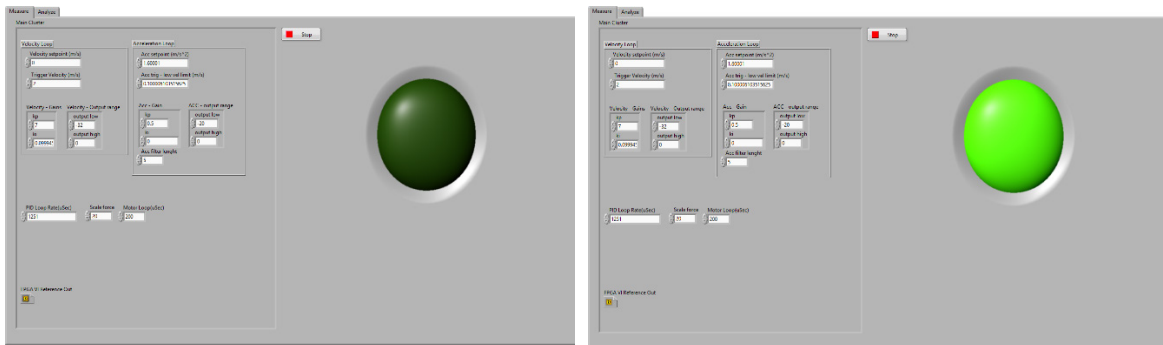
Control program inactive   Control program active

Figure 4.12 Added green light for visual confirmation of the status of the program

Figure 4.13 Damage to brake pad connecting plate. (replaceable part)
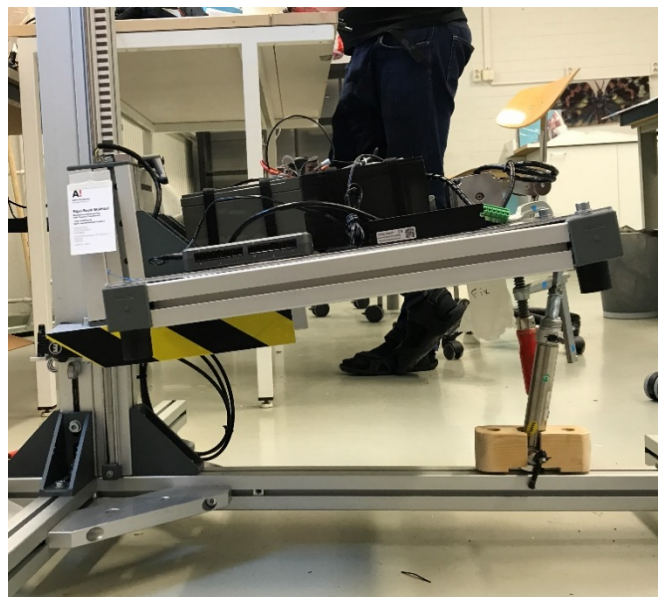
Figure 4.14: Collision with the bumper and slider slipping off
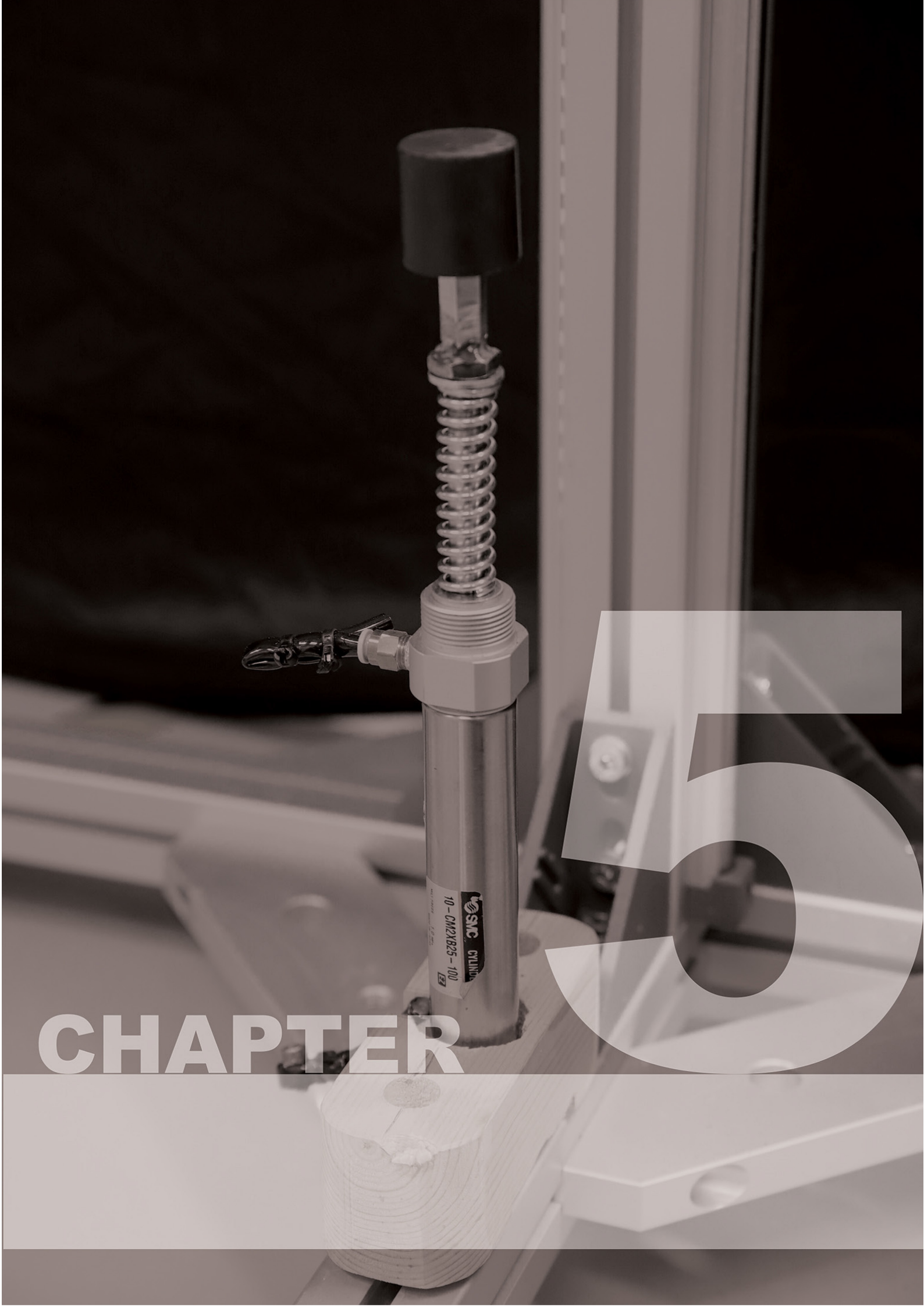
CHAPTER **5**

5   Conclusions

This chapter summarizes the results, the methods used for obtaining these results, the significance of the findings, the shortcomings of this thesis, and finally recommendation for future work.

5.1   Result Conclusions

This thesis has modeled a small-scale free-falling elevator for an intelligent safety gear system in high-rise elevators. In other words, it has taken the first steps in developing an electronically controlled safety gear system for high-rise elevators. The model was created in MATLAB Simulink, validated with a physical test rig with higher complexity than the computer model, and the results from the test rig were then compared to the those of KONE's high-rise elevator SGAT in order to verify the validity of the test rig.

Although very simple, the computer simulation was used to determine the feedback loops to be verified by the physical test rig. The computer simulation included physical properties (i.e., mass, gravity, and coefficient of frictions), an oscillator to simulate the oscillations induced by the suspension ropes, and two control feedback loops (velocity and acceleration). It was demonstrated that both the acceleration and velocity controls are essential for proper functioning of the model. The model was able to dampen the oscillations arising from the oscillator by controlling the braking force output. This level of control could not have been achieved by only using velocity control. It is, however, important to note that the model is very simplified, lacks physical properties of the motor, and only uses a PID feedback loop as the control method.

Next, a physical test rig was constructed to empirically test the free-falling mass and the brake control system. The test rig allowed a free-falling mass to drop from a maximum height of 2.5m and the brake system to halt the mass, all the while recording variables, such as velocity and acceleration. The rig proved to be very versatile and adjustable for a myriad of scenarios. Furthermore, the rig was able to mirror the results of the computer model, indicating that control of the brake based only on velocity control would not produce favorable results. For instance, when the velocity control alone was engaged, the falling mass would decelerate at a rate higher (2-2.5 Gs) than that designated by the norm EN81-2 (0.2-1G) (6). Once the acceleration control was engaged, the deceleration was controlled at the desired value of 0.6G while also successfully stopping the mass. The rig also included a physical oscillator with two possible oscillating frequencies. The physical oscillator, similar to its computer model counterpart, was added to simulate suspension rope oscillations. However, the oscillator did not prove to be effective. The oscillations induced by the oscillator were minimal and were masked by other larger amplitude vibrations. Additionally, the geared stepper motor used to actuate the brake was shown to not be sufficiently rapid in responding to vibrations and actively dampening them. At some frequencies, the motor induced vibration, because of the delay in the response to the vibrations. Moreover, the structure of the rig had some limitations, including the length of the rail, the rated load that the platform could carry, and the cantilever construction of the rig that would oscillate out of the plane of motion. Since these oscillations could not be dampened by the brake system, a more rigid structure, or alternatively, a simply supported structure are recommended as next steps in the development of a testing rig.

5.2 Future Work

This thesis recommends a number of areas for further development of the intelligent safety gear system. First, in terms of the physical test setup, the test rig could have been improved by creating a more rigid structure, as in the previous section. Furthermore, a faster motor could have been used that would have responded quicker to the vibration fluctuations and would not itself induce vibrations. In addition, the oscillator could have been improved to induce larger vibrations in order to simulate the ropes better.

A second area for further development is improving the computer model. The simulation should be modeled by employing further details, such as the physical properties of the motor (inertia, lag, force output range) and ramped acceleration, instead of a constant value. Furthermore, different methods of feedback could be used that would respond faster than PID. In addition, predictive logic could be added to the simulation, as this would change the parameters by obtaining information from stimuli other than velocity or acceleration.

Even though a small-scale test setup can be valuable, full-scale elevator tests are even better, since the brake system can be tested in a real environment alongside other elevator components. Full-scale elevator tests should add "intelligence" to the control system in order to further smoothen the braking event as a means to ensure the safety of elevator passengers. The flexibility of such an intelligent system would allow for more functions to be added to the brake, such as detecting the location of the car in the shaft and stopping the elevator at a landing to unload the passengers if deemed safe, as well as deceleration at a very low rate if there is enough room in the shaft to smoothen the deceleration and stop.

A future developed brake system could also be used in normal operation braking events, in addition to the motor brake. This would allow for more control over the location of the car, thus mitigating the need of additional suspension ropes for stiffness, as well as promoting cost savings.

Ideally, the electronic control algorithm for a future brake system could be coupled with existing guide rail brake actuator solutions, such as Patents 1, 2, &3 (Appendices Appendix 1Appendix 2Appendix 3). For example, Patents 1 and 2(Appendices Appendix 1Appendix 2) (22) (23) disclose self-contained hydraulic brake systems with feedback that would stop the car by applying brakes on the guide rails. The self-contained system ensures stopping in rare cases of total suspension loss. Additionally, the independence of the braking system from the ropes would allow more precise control of the car in the shaft. Patent 3 (Appendix 3) (24) offers a similar solution that additionally enables the use of electric actuators and can be coupled with the safety gear in order to be triggered in case of malfunction or in case the actuator is unable to fully stop the elevator. This option is also desirable because of the added layer of passive protection. Electronic control could also be added to wedge-type safety gears, such as Patents 5 & 6 (Appendix 5Appendix 6) (25) (26) which would result in a hybrid of electronic control and a mechanical force adjustment servo.

An ideal embodiment of an electronic controlled safety gear system would be one with adjustable parameters, a fast acting actuator that is able to quickly respond to control algorithm output to adjust the braking force. The actuator would be sized in order to stop a fully loaded elevator with the lowest deceleration rate. The system should be fail-safe to ensure that in case of malfunction, it is able to still engage and stop the elevator. And finally, the apparatus should be as simple as possible to reduce possible points of failure.

As a final thought, the computer simulations and the small-scale tests conducted in this thesis were promising and merit further development on a full scale to further increase the safety and the functionalities of the system.

References

1. *Understanding the Natural Behaviour of Elevator Safety Gears and Their Triggering.* **de Jong, Johannes.** Istanbul : IAEE, 2004.

2. **Gabel, Jason.** *CTBUH Year in Review: Tall Trends of 2016.* Chigaco : The Council on Tall Buildings and Urban Habitat, 2016.

3. **Ulrich, Carl T. and Eppigner, Steven D.** *Product Design and Development.* New York City : McGraw Hill Education, 2016. 978-0-07-802906-6.

4. **Kalliomäki, Jaakko.** Hoisting System Components. s.l. : KONE Corp., 2015.

5. **KONE Corporation.** Introsuction to Elevator Technology. Hyvinkää : s.n., 2015. TC000501eL.

6. **EUROPEAN COMMITTEE FOR STANDARDIZATION.** EN81-20. *Safety Rules for the Construction and Installation of Lifts.* Brussels : s.n., 2014. EN 81-20:2014 E.

7. **KONE Corp.** Progressive Type Safety Gear SGB06/07 and NSGB06 Service Instructions. Hevinkää : s.n., 2016. D. AS-07.04.019.

8. **Oleg Braun, Michel Peyrard.** Dependence of kinetic friction on velocity: Master equation approach. s.l. : American Physical Society, 2011. ensl-00589509.

9. **KONE Corp.** KONE Maintenance Method, MX10 / MX20 MCP Procedures - ASME A17.1-2013 / CSA B44-13. Hevinkää : s.n., 2014. PSK8-604-MX10/MX20.

10. —. Progressive Type Safety Gear SGB06/07 and NSGB06 Product Description. Hyvinkää : s.n., 2017. L. SO-07.06.012.

11. **Dorf, Richard and Bishop, Robert.** *Modern Control Systems.* s.l. : Pearson Education, Inc., 2011. 978-0-13-602458-3.

12. *Limitations and Countermeasures of PID Controllers.* **Sung, Su Whan and Lee, In-Beum.** s.l. : ACS Abstracts, 1996. IE960090+.

13. **PID Feedback Loop.** *Wikipedia.* **[Online] [Cited: 10 13, 2017.] (https://en.wikipedia.org/wiki/File:PID-feedback-loop-v1.png).**

14. **Sliding Guides, Part 2: Linear Bushings vs. Linear Guides.** *MisumiUSA.com.* **[Online] Misumi. [Cited: 11 07, 2017.] http://blog.misumiusa.com/sliding-guides-part-2-linear-bushings-vs-linear-guides/.**

15. **What are recirculating linear bearings?** *LinearMotionTips.com.* **[Online] [Cited: 11 07, 2017.] http://www.linearmotiontips.com/faq-what-are-recirculating-linear-bearings/.**

16. **myRIO Student Embedded Device.** *ni.com.* **[Online] National Instruments Inc. [Cited: 11 27, 2017.] http://www.ni.com/en-us/shop/select/myrio-student-embedded-device.**

17. **National Instruments Inc. User Guide and Specifications NI myRIO-1900. Austin : National Instruments, 2016.**

18. **LabVIEW Environment Basics.** *ni.com.* **[Online] National Istrument Inc. [Cited: 11 27, 2017.] http://www.ni.com/getting-started/labview-basics/environment.**

19. **NI FPGA.** *ni.com.* **[Online] National Instruments Inc. [Cited: 11 27, 2017.] http://www.ni.com/fpga/.**

20. **FPGA or GPU? - The evolution continues.** *mil-embedded.com.* **[Online] [Cited: 11 27, 2017.] http://mil-embedded.com/articles/fpga-gpu-evolution-continues/.**

21. **ISO. NEN-ISO 18738-1.** *Measurement of ride quality - Part 1: Lifts.* **Switzerland : s.n., 2012. E.**

22. **Karl Kriener, René Holzer, Marlene Rechberger, Peter Ladner, Bernd Winkler, Karl Ladner.** *Hydraulic Elevatror Car Brake Unit with Controllable Braking Power. WO 2015/177228 A1* **Germany, 11 26, 2015.**

23. **Nigel, Heinz-Dieter.** *Brake Regulating Apparatus for an Elevator Car. US 5,648,644* **USA, 07 15, 1997.**

24. **Harold Terry, Leandre Adi-fon, Richard N. Fargo, Da-vid J. Lanesey, Anthony Cooney, James M. Draper, Jamie A. Rivera, Justin Billard, Zbigniew Piech.** *Elevator Braking System. US 2014/0008157 A1* **USA, 01 09, 2014.**

25. **Mineo, Okado.** *Elevator Safety Device. EP2517998A1* **Germany, 12 15, 2004.**

26. **Oliver Simmonds, Stefan Hugel, Julien Maury, Peter Mori, Peter Aeschlimann.** *Brake Arresting Device with Adaptable Brake Force for an Elevator. US 2003/0085078 A1* **USA, 05 08, 2003.**

27. **Takuo Kugia, Kenichi Okamoto, Takashi Yumura, Mineo Okada.** *Elevaor Apparatus with Position Correction for Overspeed Detection. US 7,228,943 B2* **USA, 06 12, 2007.**

Table of Figures

Appendices

Appendix 1

Name:	**Hydraulic Elevator Car Brake Unit with Controllable Braking Power**	Inventors:	Karl Kriener, René Holzer, Marlene Rechberger, Peter Ladner, Bernd Winkler, Karl Ladner
Patent number:	WO 2015/177228 A1		
Publication date:	26/11/2015	Assignee:	WITTUR HOLDING GMBH
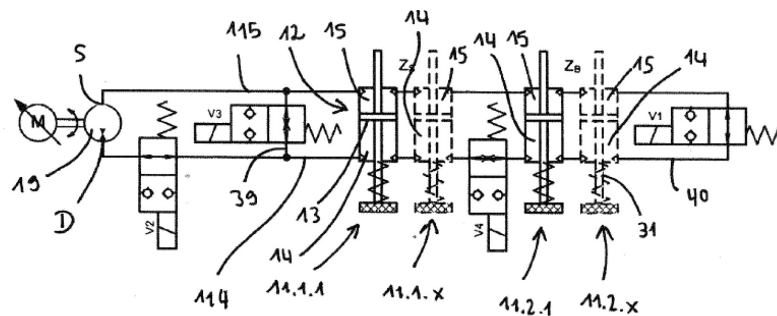
Figure APP 1.0.1 Hydraulic Elevator Car Brake Unit with Controllable Braking Power
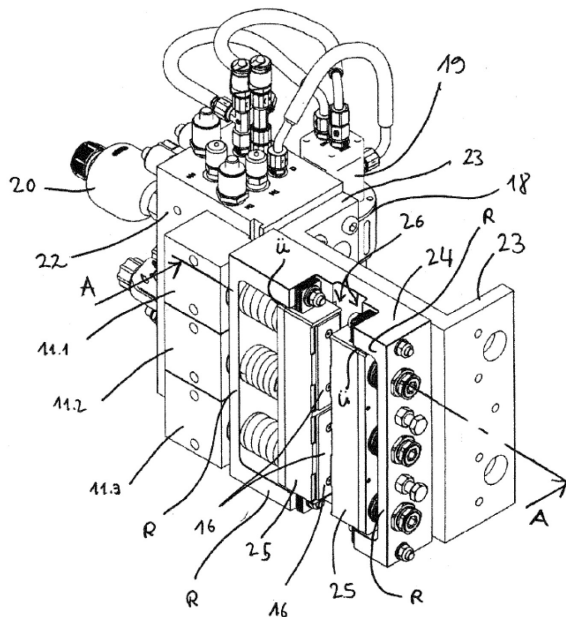
Figure APP 1.0.2: Self-contained unit

In this patent, a hydraulic system is disclosed that is able to control and decelerate the elevator. This system could be coupled with an open or closed loop feedback system. An embodiment of the invention is a self-contained brake device. (22)

Appendix 2

Name:	**Brake Regulating Apparatus for an Elevator Car**	Inventors:	Heinz-Dieter Nagel
Patent number:	US 5,648,644	**Assignee:**	INVENTIO AG, Hergiswil, Switzerland
Publication date:	15/07/1997		
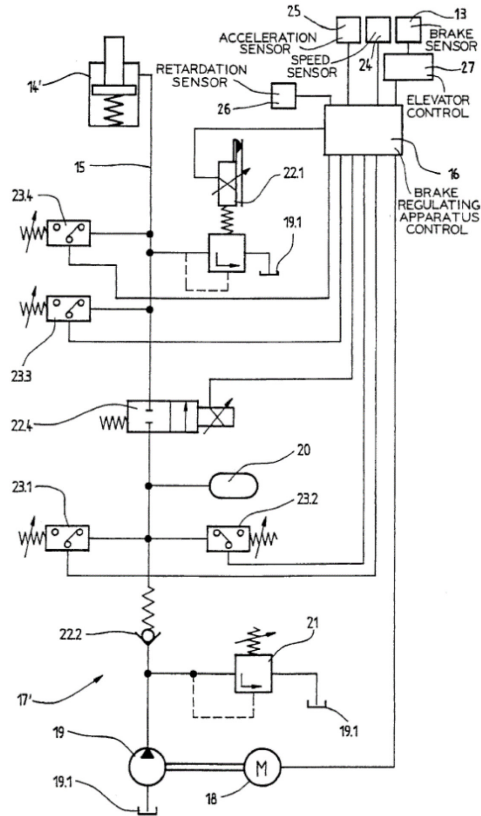
Figure APP 2.0.3: Brake Regulating Apparatus for an Elevator Car

In this patent, a hydraulic system with feedback is disclosed that is able to control and decelerate the elevator independent of the direction of travel. This apparatus aims to maintain a constant deceleration of the car and promote "travel comfort and safety even in the case of emergency braking, and in particular for disabled users of the elevator." (23)

Appendix 3

Name:	**Elevator Braking System**	Inventors:	Harold Terry, Leandre Adifon, Richard N. Fargo, David J. Lanesey, Anthony Cooney, James M. Draper, Jamie A. Rivera, Justin Billard, Zbigniew Piech
Patent number:	US 2014/0008157 A1		
Publication date:	09/01/2014	Assignee:	OTIS ELEVATOR COMPANY

Figure APP 3.0.4: Elevator braking system

Figure APP 3.0.5: Elevator brake system in conjunction with a SG
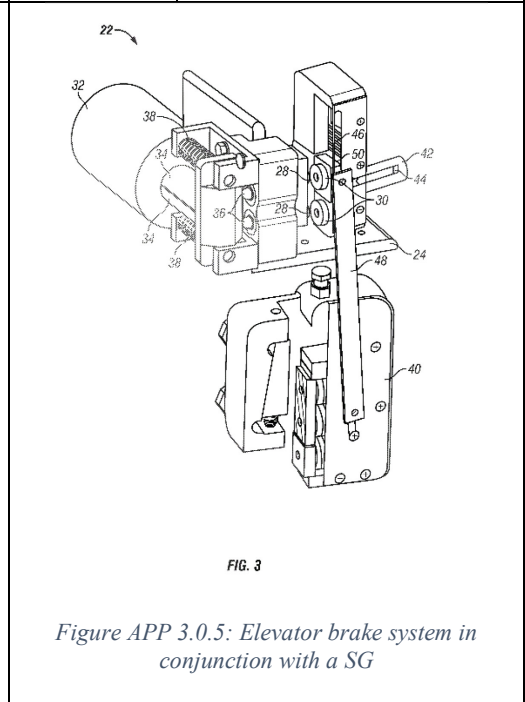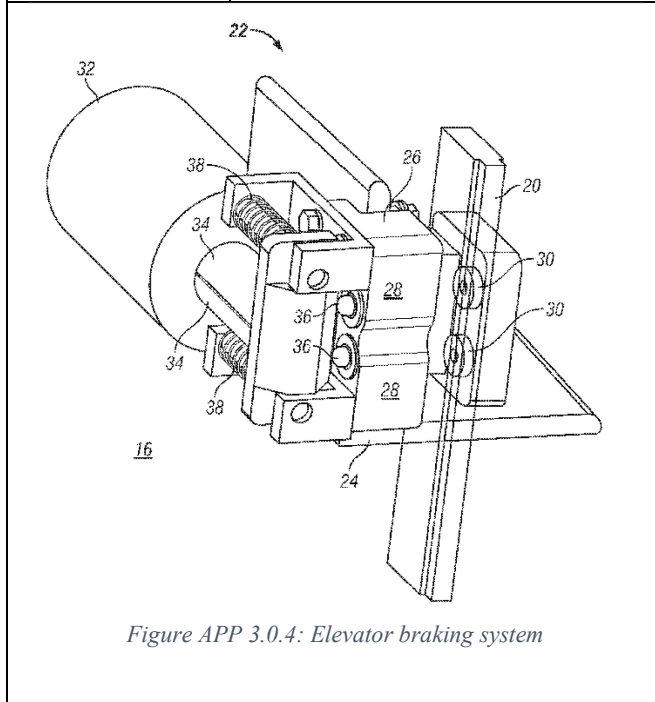
In this patent, a guide rail braking system is disclosed that controls or stops the moving car by applying brake surfaces to the guide rails. The brake surfaces can be actuated by a solenoid, linear motor, or other types of actuators. This invention can be used in conjunction with an SG where the addition of a safety plunger and trip rod can engage and disengage the SG. (24)

Appendix 4

Name:	**Elevator Apparatus with Position Correction for Overspeed Detection**	Inventors:	Takuo Kugia, Kenichi Okamoto, Takashi Yumura, Mineo Okada
Patent number:	US 7,228,943 B2		
Publication date:	12/06/2007	Assignee:	MITSUBISHI DENKI KABUSHIKI KAISHA
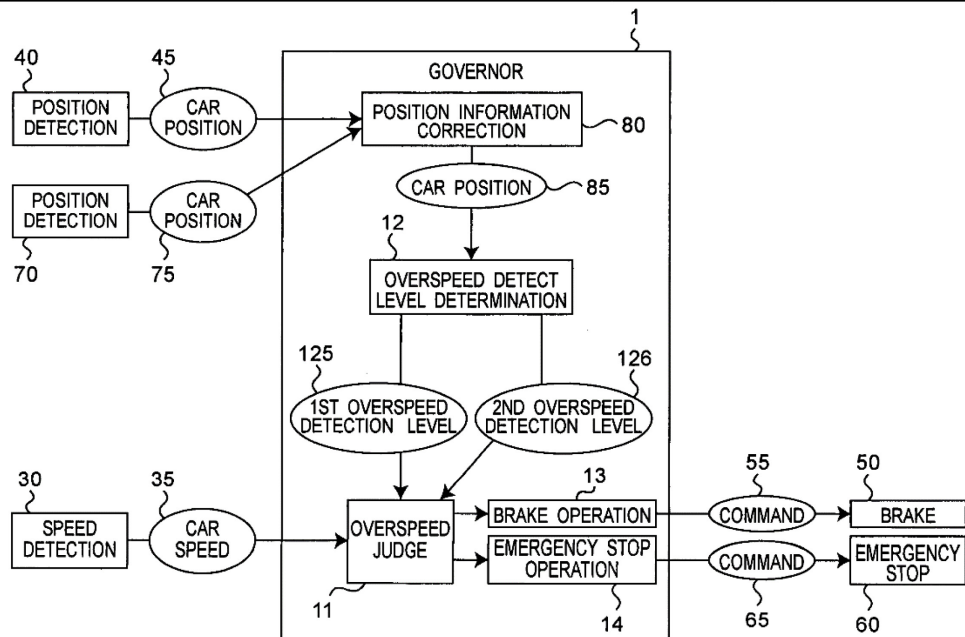
Figure APP 4.0.6: Elevator Apparatus with Position Correction for Overspeed Detection

In this patent, an apparatus is disclosed which is able to continuously measure the velocity of the elevator and correct it by periodic measurements of distance. This apparatus can enable dynamic adjustment of overspeed trigger velocity and actuate brakes if necessary. (27)

Appendix 5

Name:	**Elevator Safety Device**	Inventors:	Okada Mineo
Patent number:	EP2517998A1		
Publication date:	15.12.2004	Assignee:	MITSUBISHI ELECTRIC CORPORATION
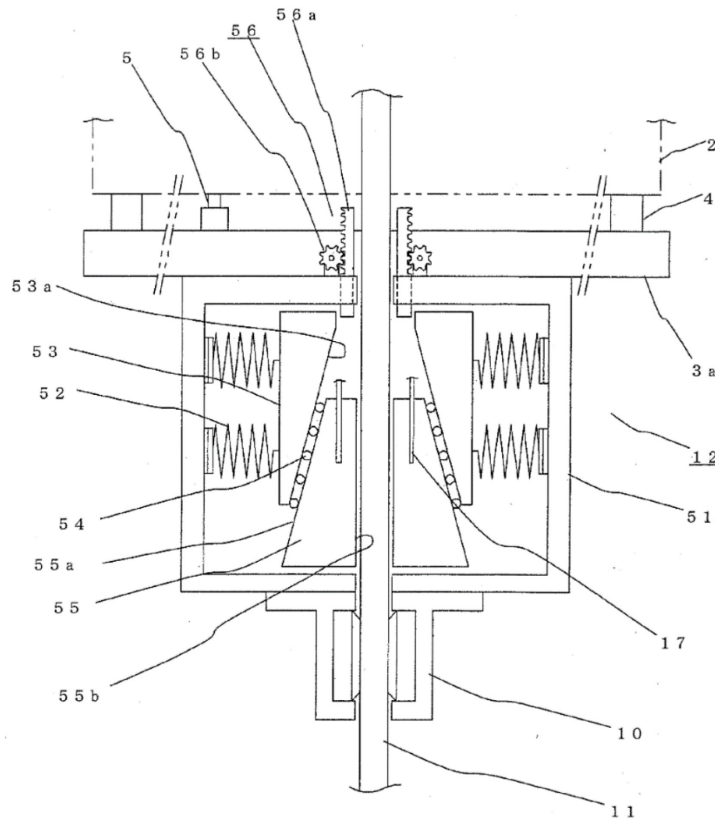
Figure APP 5.0.7: Elevator safety device

In this patent, a device is disclosed which consists of safety wedges that reduce deceleration during braking operation. The braking force can be set remotely in the beginning of braking event; however, it cannot be changed dynamically. Mechanical servo type. (25)

Appendix 6

Name:	**Brake Arresting Device with Adaptable Brake Force for an Elevator**	Inventors:	Oliver Simmonds, Stefan Hugel, Julien Maury, Peter Mori, Peter Aeschlimann
Patent number:	US 2003/0085078 A1		
Publication date:	08/05/2003	Assignee:	INVENTIO AG
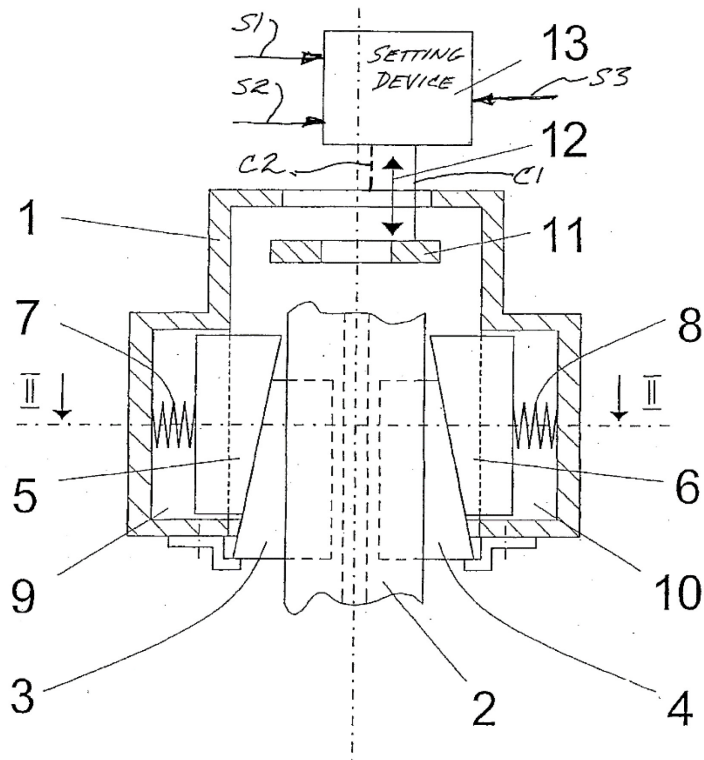
Figure APP 6.0.8: Brake Arresting Device with Adaptable Brake Force for an Elevator

In this patent, similar to EP2517998A1, a device is disclosed which uses wedge type brakes and a setting device to actively (i.e. with a servo motor) control the deceleration of the elevator based on the moving mass. Mechanical servo type. (26)

Appendix 7: LabVIEW Control Program

Motor control

GUI
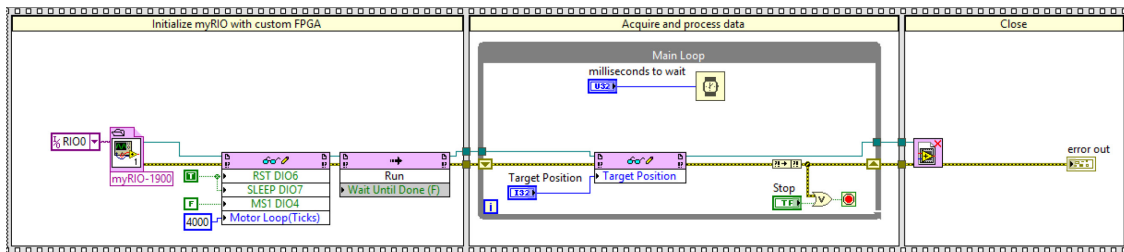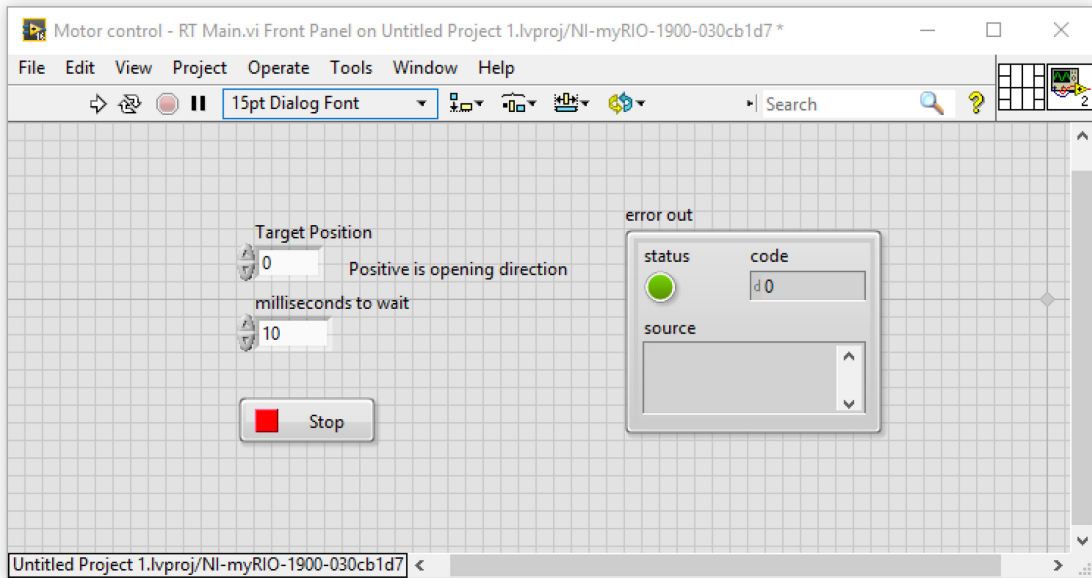
FPGA
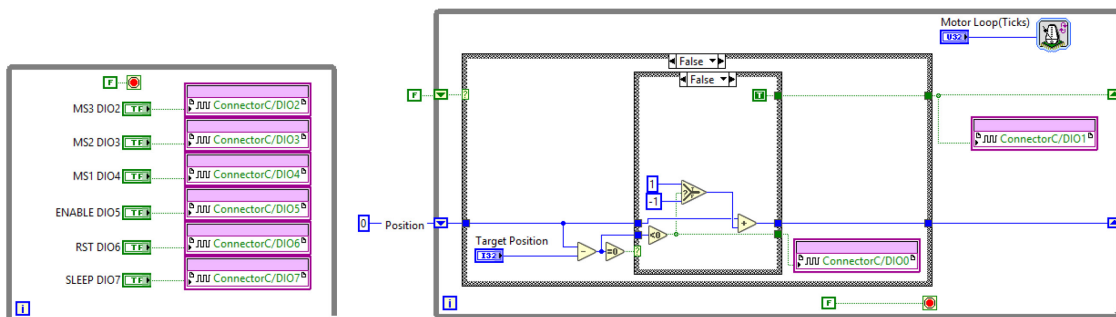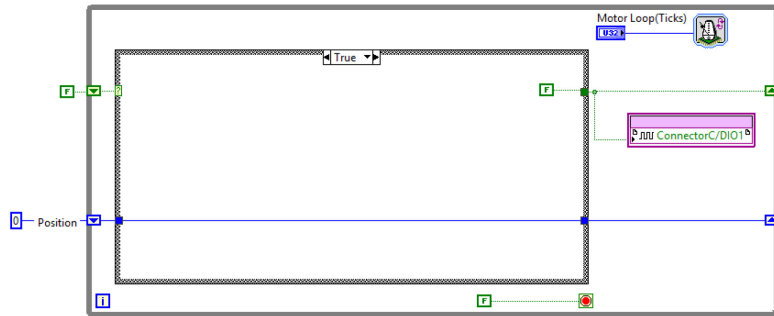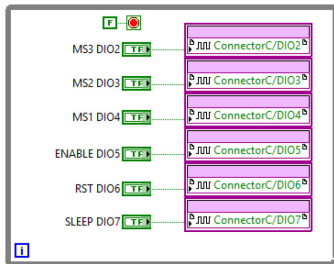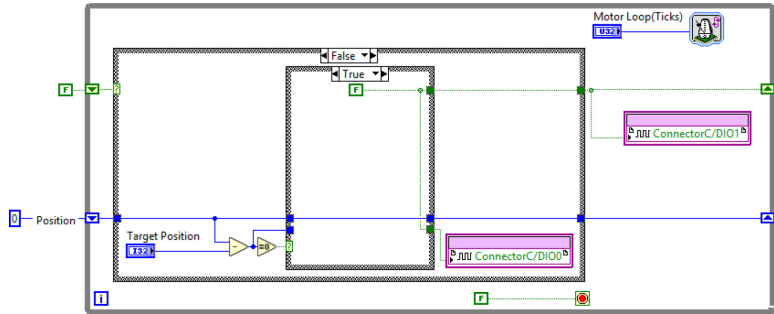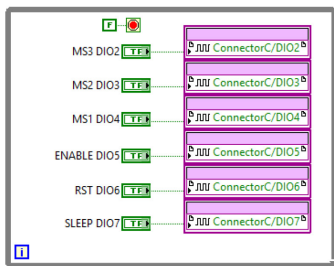
Motor control Velocity & acc Loop - RT Main

GUI

Measure Analyze

Main Cluster

Velocity Loop

Velocity setpoint (m/s)
0

Trigger Velocity (m/s)
2

Acceleration Loop

Acc setpoint (m/s^2)
1.60001

Acc trig - low vel limit (m/s)
0.100006103515625

Velocity - Gains
kp
7
ki
0.09994

Velocity - Output range
output low
-32
output high
0

Acc - Gain
kp
0.5
ki
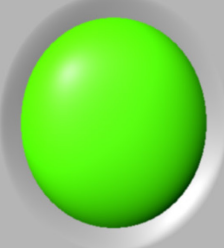
ACC - output range
output low
-20
output high
0

Acc filter lenght
5

Stop

PID Loop Rate(uSec)
1251
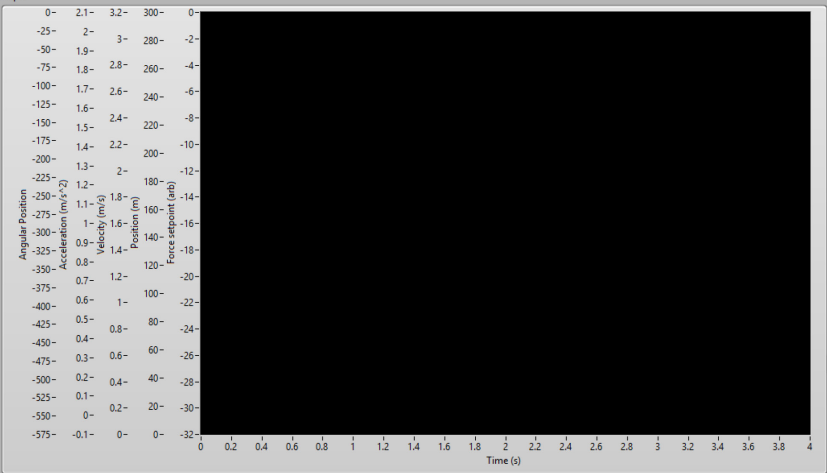
Scale force
20

Motor Loop(uSec)
200

FPGA VI Reference Out

Measure Analyze

Graph

Angular Position
Acceleration (m/s^2)
Velocity (m/s)
Position (m)
Force setpoint (arb)

Time (s)

☑ Position
☑ Velocity
☑ Acceleration
☐ Vel Force Setpoint
☐ Acc Force Setpoint
☐ Trigger vel
☐ Trigger low vel level
☐ Force setpoint
☐ Target Position
☑ Current Position

Cursors: X Y
Cursor 0 0 0

EXIT

11

FPGA

Front Panel
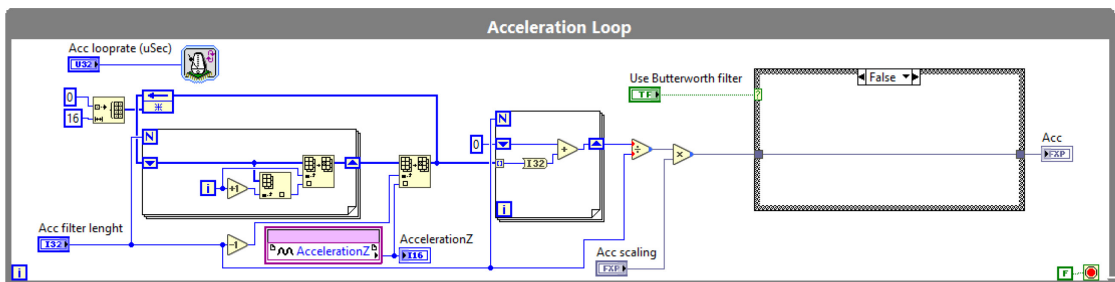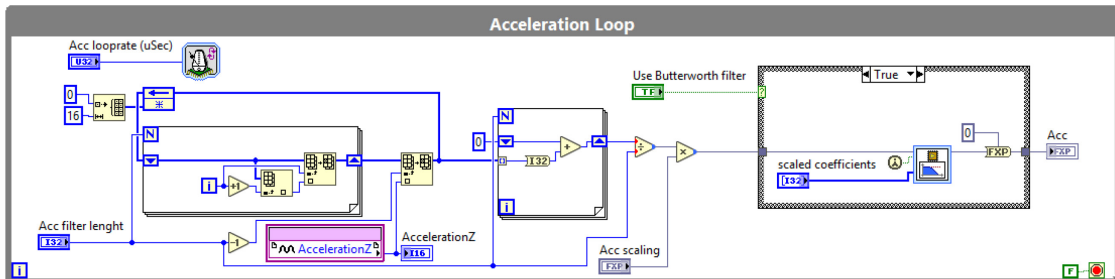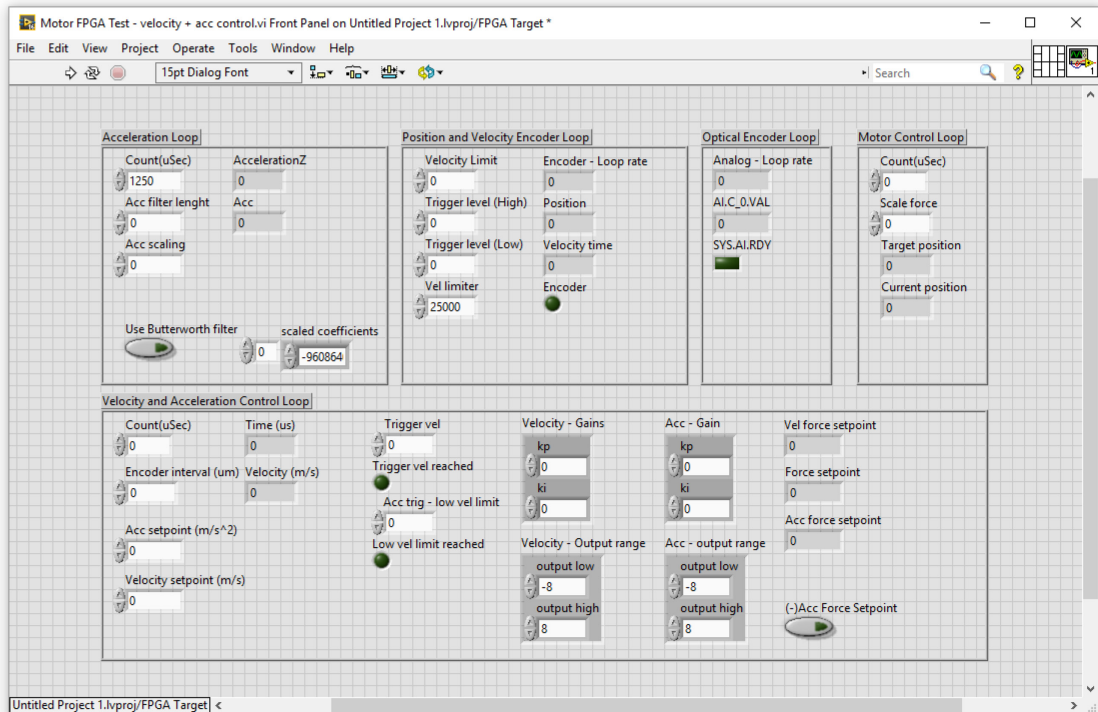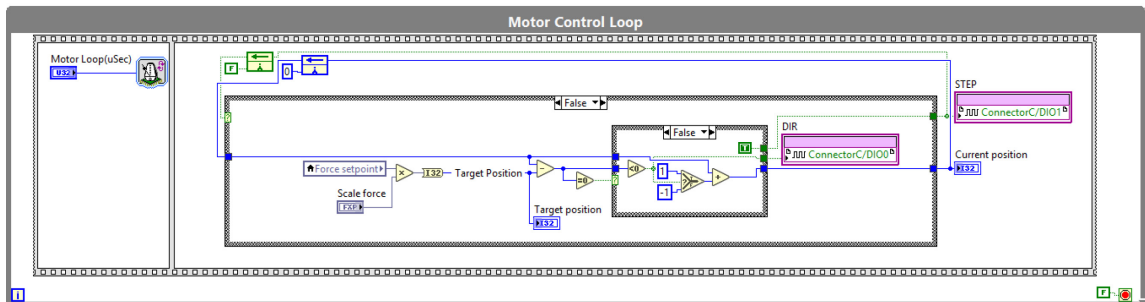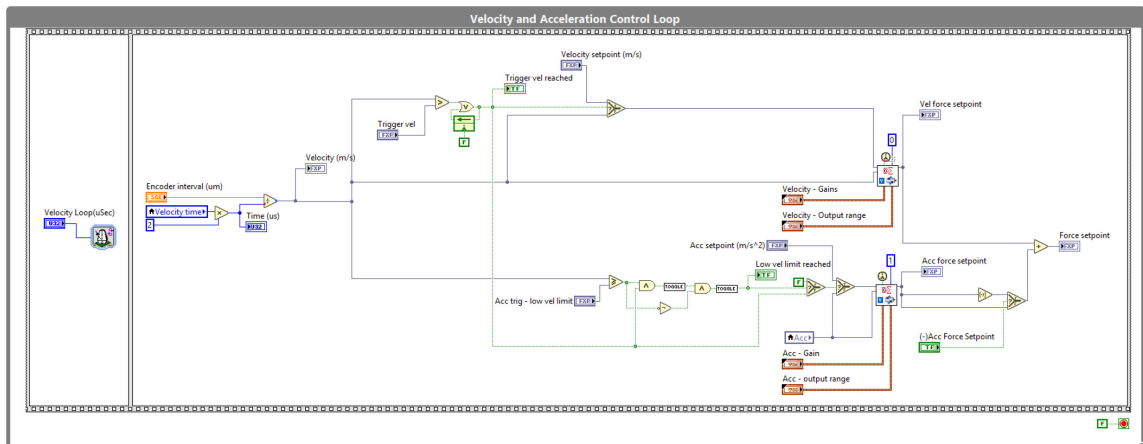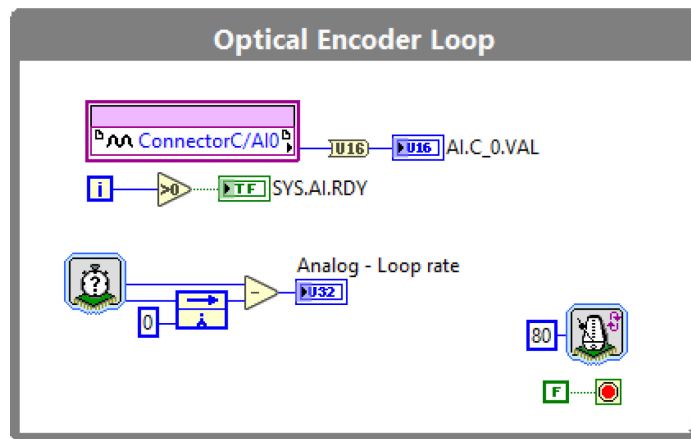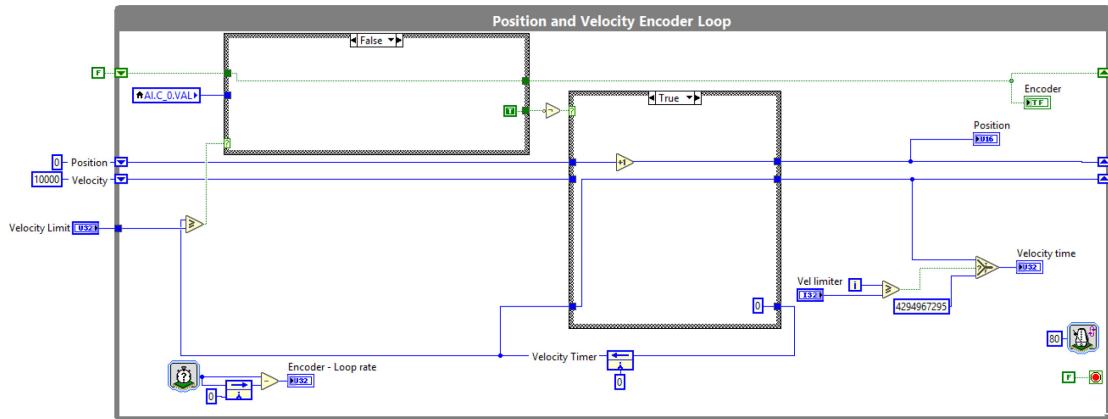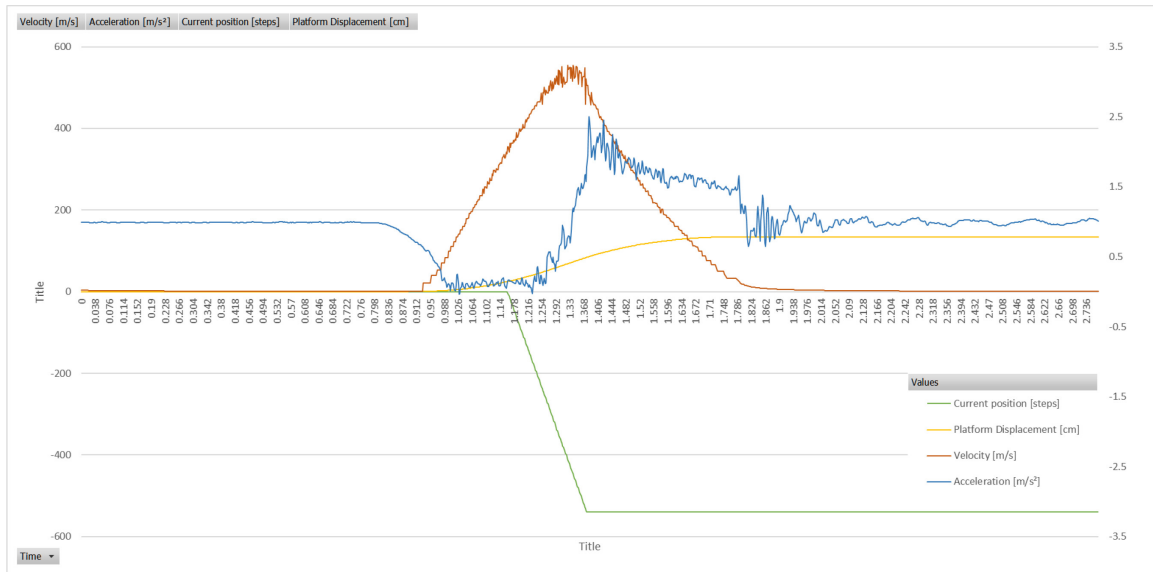
Appendix 8: Physical Test Rig Results

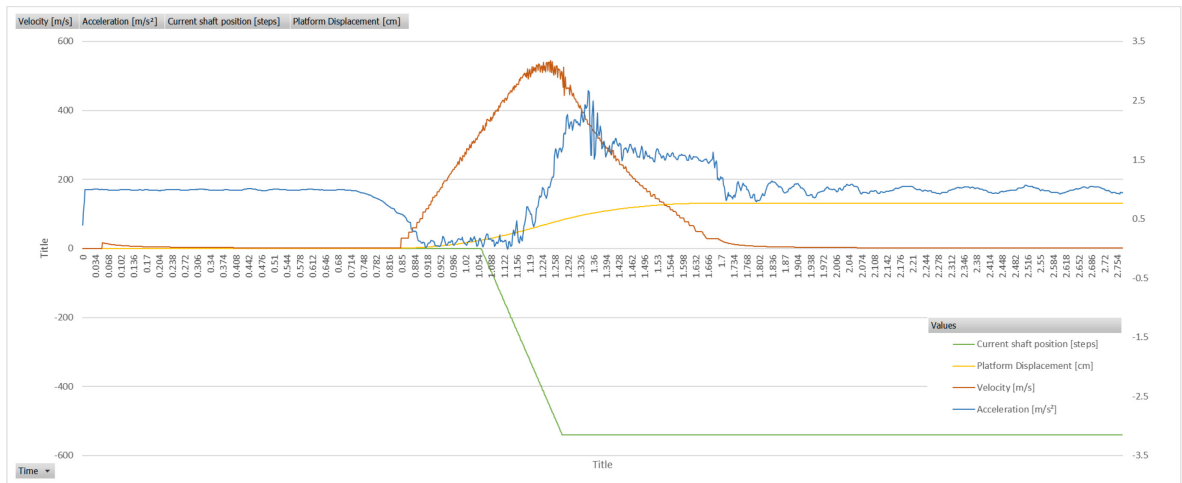*Figure 0.9 Constant force soft spring oscillator*

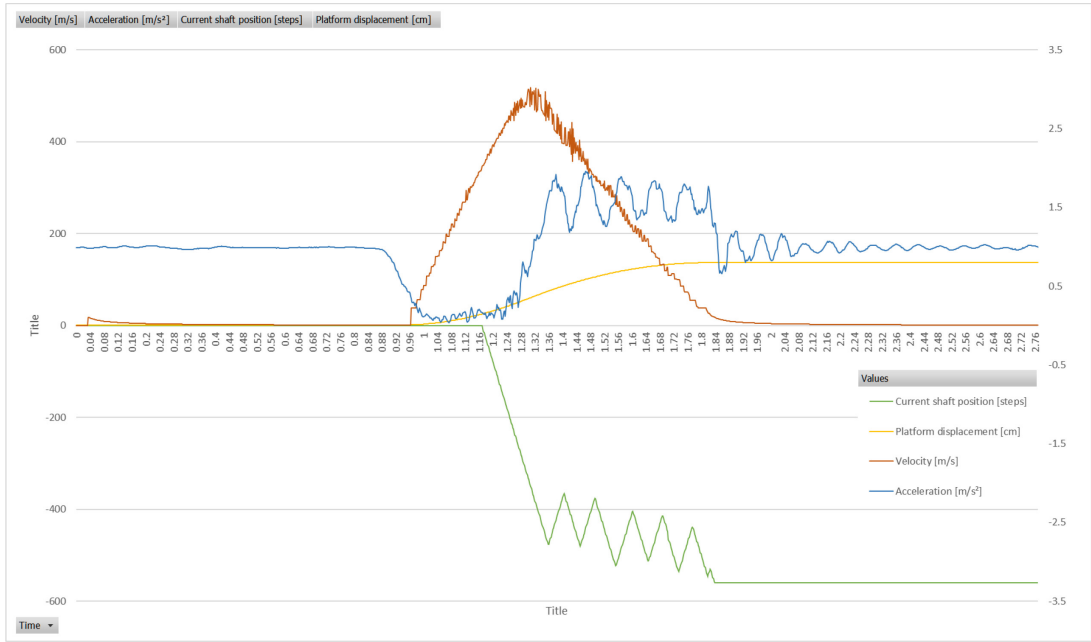*Figure 0.10 Constant Force stiff oscillator*

15

Figure 0.11 Velocity and acceleration control
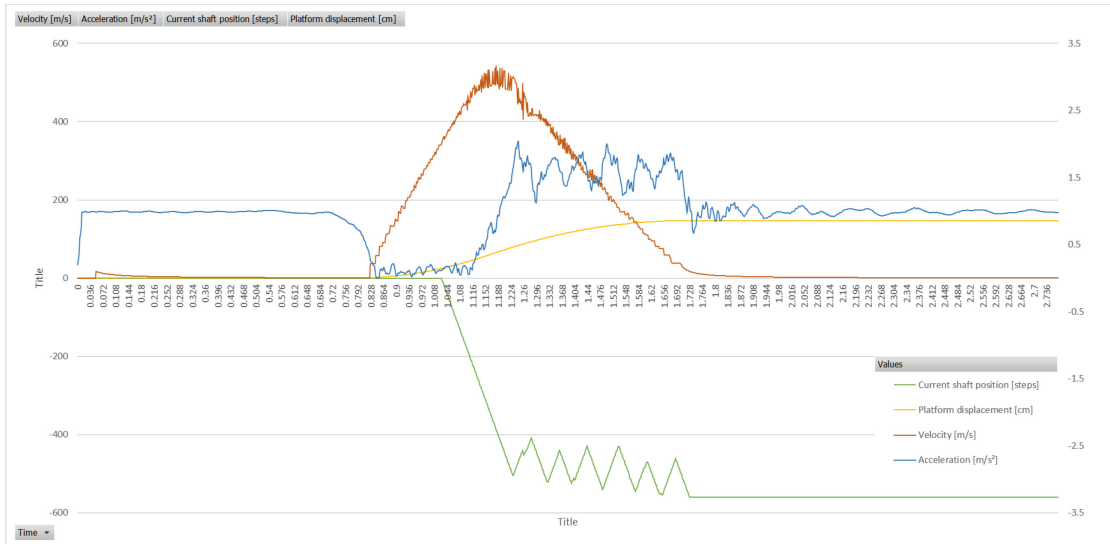

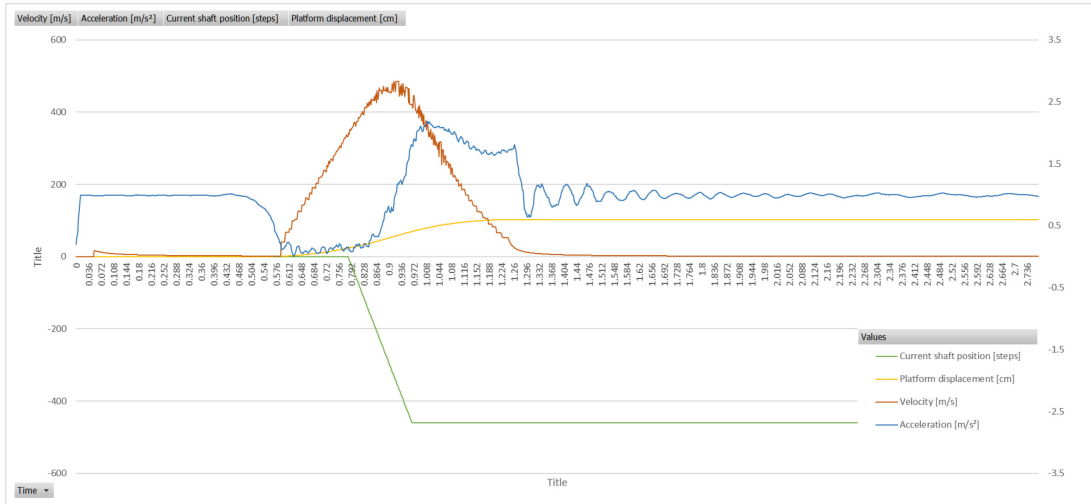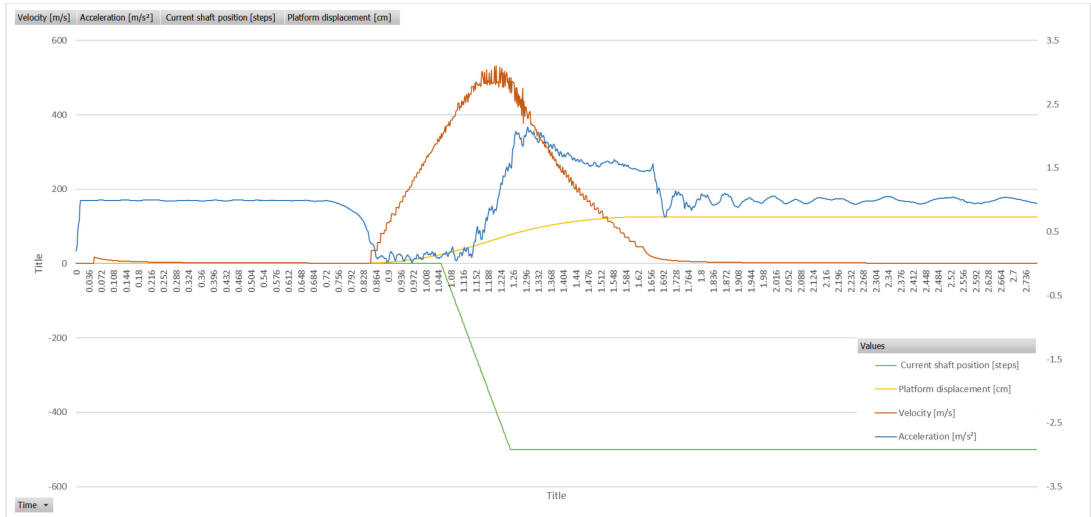*Figure 0.12 Velocity and acceleration control with soft oscillator*

Figure 0.13 Velocity control

Figure 0.14 Velocity control soft oscillator

17